STUDY OF HEAT TRANSFER OF EVAPORATING FREON--12 IN HORIZONTAL TUBE EVAPORATOR

BY

BRIJENDRA KUMAR STHAPAK

A
THESIS SUBMITTED IN PARTIAL
FULFILMENT OF REQUIREMENTS FOR THE DEGREE
OF

Master of Engineering

IN

Applied Thermodynamics

(Refrigeration & Airconditioning)

DEPARTMENT OF MECHANICAL ENGINEERING
UNIVERSITY OF ROORKEE
ROORKEE (INDIA)

JUNE, 1964

C E R T I F I C A T E

CERTIFIED that the dissertation entitled "STUDY OF HEAT-TRANSFER OF EVAPORATING FILMS IN HORIZONTAL TUBE EVAPORATOR" which is being submitted by Sri Brijendra Kumar Sthapak in partial fulfilment for the award of the Degree of Master of Engineering in Applied Thermodynamics (Refrigeration and Air-Conditioning) of University of Roorkee is a record of student's own work carried out by him under my supervision and guidance. The matter embodied in this dissertation has not been submitted for the award of any other Degree or Diploma.

This is further to certify that he has worked for a period of nine months from 15th September, 1963 to 15th June, 1964 for preparing dissertation for Master of Engineering Degree at the University of Roorkee.

Dated June 23 1964

Rajendra Prakash

(Rajendra Prakash)
Reader in Mechanical Engg.
University of Roorkee, Roorkee.

ACKNOWLEDGEMENTS

The author expresses his deep and sincere gratitude to Shri Rajendra Prakash, Reader in Mechanical Engineering, University of Roorkee and Dr. T.U.Price, U.S.A.I.D. Guest Professor in Mechanical Engineering at the University of Roorkee for their valuable guidance and expert advice in preparation of this investigation.

The author is also indebted to Prof. H.V.Kamlani, Head of Mechanical Engineering Department, University of Roorkee for his constant encouragement.

The assistance given by the staff of Refrigeration and Heat-Transfer Laboratory during setting-up of the apparatus and its testing is highly appreciated.

ABSTRACT.

The work presented here comprises of the theoretical background of the topic and an experimental investigation of various aspects of it. Though the name of the topic "Study of Heat Transfer of Evaporating Freon-12 in a Horizontal Tube Evaporator" does not refer to inclined tube, the author has also dealt with evaporator tube inclined at small angles to horizontal. The first three chapters deal with the mechanism of bubble formation Heat transfer during evaporation and vaporisation inside horizontal tube respectively, where the various approaches put forward by different investigators have been discussed. The last two chapters deal with the experimentation part of the work, a test set-up has been sought, designed and tested. The results thus obtained have been discussed and some interesting conclusions drawn in the end.

C O N T E N T S

INTRODUCTION

Evaporation is quite a general process. Whenever a liquid surface is in contact with a gaseous environment, molecules leave the liquid surface and mix up with the gas. Evaporation from inside a liquid body under the formation of vapour bubbles is called boiling. Heat transfer to boiling occurs in several kinds of heat exchange apparatuses. The most common examples are steam boilers and the evaporators of refrigerating plants and chemicals industries.

Inspite of the wide use of equipment of this sort and even with the fact that extensive studies have been and are being made of the heat transfer in this equipment, the information developed concerning the heat transfer to boiling liquids is still far from complete or satisfactory.

Heat transfer to boiling liquids is a convection process involving a change in the phase from liquid to vapour. The phenomenon of boiling heat transfer are considerably more complex than those of convection without phase change, because in addition to all other variables associated with convection, those associated with change of phase are also relevant. As seen in the liquid phase convection, the geometry of the system,

the viscosity , the density, the thermal conductivity, the expansion coefficient and the specific heat of the liquid are sufficient to describe the process. Whereas in the boiling heat transfer, the surface characteristics, the surface tension, the latent heat of vaporization, the pressure, the density and possibly other properties of vapor also play an important part. As a result of large number of variables involved neither general equations describing the boiling process nor general correlations of boiling heat transfer data are available uptodate.

The purpose of this work is

a) To make an extensive study of the mechanism of vaporisation and,

b) To co-relate the heat transfer, pressure drop data for a vaporizing liquid as well as to study the the local heat transfer coefficients. The vaporizing liquid selected for this work is Freon$_{-12}$ as it is the most commonly used refrigerant in the refrigeration applications.

The problem of heat transfer rates of evaporating Freon$_{-12}$ is of great significance these days due to increasing emphasis being laid on the optimization of evaporators. Air-borne refrigerant evaporators in particular have placed a premium on minimum size and

weight. An improved knowledge of local evaporating heat transfer and pressure drop is therefore mendatory before the optimization can be accomplished.

As most of the cooling coils of the refrigeration plants are made horizontal, therefore heat transfer rates of vaporizing $Freon_{-12}$ in horizontal tube are of practical value. Any inclination of the tube to the horizontal would certainly affect the heat transfer rates. The experimental investigation in this work aims at exploring the heat transfer rates mainly in a horizontal tube. However effect of varying the tube angle on heat transfer has also been studied.

NOMENCLATURE

A	Total heat transfer (L^2)
a	Thermal diffusivity ($L^2\,\theta^{-1}$)
C_L	Specific heat of liquid at constant pressure.
D	Diameter of bubble (L)
D_b	Diameter of a bubble departing from a heated horizontal surface (L)
d_o	Diameter of cavity on the Heating surface (L)
f	Frequency of bubble emission (θ^{-1})
G	Acceleration due to gravity ($L\theta^{-2}$)
h_{fg}	Latent heat of vaporisation (HM^{-1})
t_b	Bubble break-off time (θ)
T_w	Absolute temperature of solid.
T_{sat}	Absolute saturation temperature.
U_t	Terminal velocity of bubble rise ($L\theta^{-1}$)
ρ_L	Density of liquid (ML^{-3})
ρ_v	Density of vapour (ML^{-3})
σ	Surface tension ($M\theta^{-2}$)
θ	Contact angle in degrees.

CHAPTER -I

PHENOMENON OF VAPORIZATION

The physical interpretation of boiling regimes have been dealt here. The nucleate boiling has been presented from the fluid flow and heat-transfer aspects, discussing the mechanism of bubble formation. The various factors affecting the nucleate boiling have been discussed in the end.

NOMENCLATURE

A	Total heat transfer (L^2)
a	Thermal diffusivity ($L^2\,\theta^{-1}$)
C_L	Specific heat of liquid at constant pressure.
D	Diameter of bubble (L)
D_b	Diameter of a bubble departing from a heated horizontal surface (L)
d_e	Diameter of cavity on the Heating surface (L)
f	Frequency of bubble emission (θ^{-1})
g	Acceleration due to gravity ($L\theta^{-2}$)
h_{fg}	Latent heat of vaporization (HM^{-1})
t_b	Bubble break-off time (θ)
T_w	Absolute temperature of solid.
T_{sat}	Absolute saturation temperature.
U_t	Terminal velocity of bubble rise ($L\theta^{-1}$)
ρ_L	Density of liquid (ML^{-3})
ρ_v	Density of vapour (ML^{-3})
σ	Surface tension ($M\theta^{-2}$)
ϕ	Contact angle in degrees.

The process of vaporisation , as considered here, results in the conversion of a liquid into vapour. The evaporation associated with the transfer of heat from a solid wall to the fluid is of primary interest.

In general, the processes and data for heat transfer associated with evaporation have not been adequately described and correlated. They are grouped according to the nature of the fluid motion and according to the physical disposition of the heating surface. The various types of heating surfaces are:-

1. Horizontally submerged flat plates.
2. Vertically submerged tubes or plates.
3. Horizontally submerged tubes.
4. Inside surface of a tube with fluid flowing therein.

The various types of resulting fluid motion are,

1. Evaporation without boiling.
2. Nucleate Boiling.
3. Film Boiling.

If the liquid is greatly subcooled the processes of evaporation by boiling may occur locally at the heating surface and be accompanied by subsequent condensation in the colder bulk of the fluid, resulting in no net evaporation.

~~evaporation~~.

In discussing the evaporation processes there are three important magnitudes to consider t_w, temp of the heating surface at the liquid solid interface, t_{sat}, the saturation temperature or the boiling point of the liquid, corresponding to the pressure, and t_{liq}, the temperature of liquid being evaporated.

In the ordinary boiling of water at its saturation temp, evaporation occurs at the free surface without the formation of bubbles when the heating surface temperature, t_w is only a few degrees above saturation temp, t_{sat}. As the temp. differential i.e. $t_w - t_{sat}$ is increased vapour bubbles form and agitate the liquid in the vicinity of the heating surface. This type of boiling is called nucleate boiling, the details of which shall be discussed later. Eventually with the increase in temperature differential , the amount of heating surface covered with vapour bubbles is increased until the entire free surface becomes "vapour blanketed". This results in a process called " film boiling".This usually does not occur in refrigerators.

1.1 EVAPORATION ON A FREE LIQUID SURFACE WITHOUT BOILING.

Using distilled, degasified water in a clean glass container, Heidrich investigated the temperature

distribution on heat flow rates in evaporating water without boiling. The resulting temperature distribution and the heat flow rate curves are shown in Fig. 1.1.

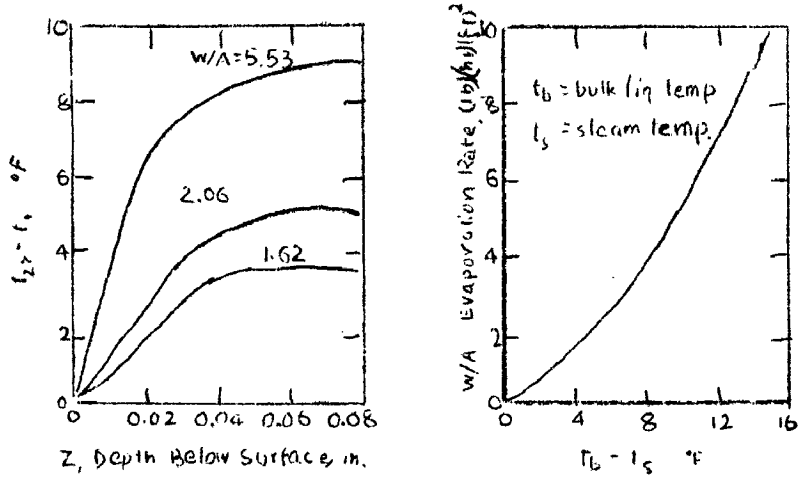

FIG 1.1 EVAPORATION WITHOUT BOILING.

It is observed that near the surface the temp gradient is very nearly linear, suggesting a stagnant layer in which heat is transferred by conduction alone. Below this layer temperature is nearly constant with depth, suggesting existence of convection currents which tend to equalise the temperatures. The rate of evaporation, which is a measure of the rate of heat transfer, increases more rapidly at higher values of $t_{l,b} - t_{st}$. This effect is accompanied by a decrease in thickness of the apparently stagnant surface layer due to an increased natural convection below the surface layer, since the heat added at the walls of the container produces a less dense fluid at the bottom.

1.2 REGIMES IN BOILING.

By observing the boiling phenomenon with the aid of high speed photography, it has been found that there are various distinct regimes of boiling in which heat transfer mechanism differ radically. Experiments in pool boiling with an electrically heated wire submerged horizontally in a tank of water at saturation temperature have been reported by Farber and Scorah[1] and McAdams[2]. The resulting characteristic curve in Fig. 1.2. illustrates the various regimes.

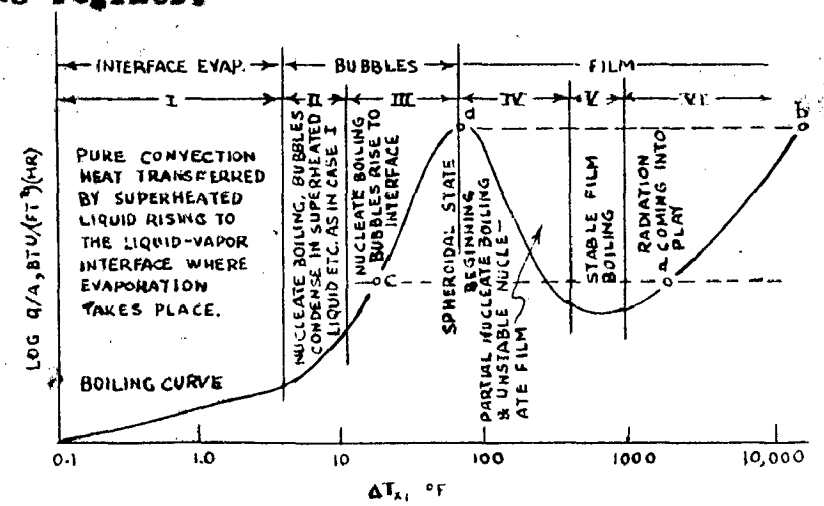

FIG. 1.2. PHYSICAL INTERPRETATION OF BOILING CURVE.

I- Pure convection: Heat transferred by superheated liquid rising to liquid-vapour interface where evaporation takes place.

II- Nucleate boiling- Bubbles condense in superheated liquid as in Case 1.

III- Nucleate boiling- Bubbles rise to interface.

IV- Spherodial state beginning: Partial nucleate boiling and unstable nucleate film.

V- Stable film boiling.

VI- Radiation coming into play.

As the wall temperature rises above the saturation temperature, convection currents circulate the superheated liquid and vapour is produced by evaporation at the free surface. Further increase in surface temp is accompanied by the formation of vapor bubbles which rise at the favored spots on the metal surface and condense before reaching the free surface. In Regime III more and larger bubbles form and transport vapour to the vapour space. Beyond the peak of the curve, an unstable film forms around the wire and large bubbles are formed at the outer upper surface of the film. This film is not stable and under the action of circulation currents it collapses and reforms rapidly. The presence of this film provides an additional resistance to heat transfer and reduces the heat transfer rate. For higher values of ΔT_x the vapour film round the wire is stable in the sense that it does not collapse and reform repeatedly, but the shape of the outer film varies continuously. For values beyond 1000^0F the influence of radiation becomes pronounced.

The characteristic curve of Fig.1.2 is obtained readily if condensing vapour heating is used, but when electrical heating is used the regime IV is difficult to obtain. As the electrical energy and hence heat flux $\frac{q}{A}$ is increased, the resulting ΔT_x increases in regime III.

When the peak value of q/A is reached, any further increase in electrical energy is accompanied by a lower q/A. The difference between these two quantities causes a rise in internal energy of wire accompanied by a further decrease in q/A. In short, the system is unstable and unless the electrical input is reduced, the system will proceed toward point b of Fig.1.2, where the wire temp is very high. Generally this temperature is above melting point for most metals, and the wire melts before reaching the point b. For this reason point a is generally referred to as the burn-out point.

NUCLEATE BOILING

For the discussion of heat transfer of evaporators used in refrigeration, the regime of nucleate boiling is of considerable significance. Before a method of correlating the heat transfer rates is sought, it is necessary to review the phenomenon of nucleate boiling. There are many experimental data concerning nucleate boiling heat transfer and also many theoretical works executed to clarify this problem. It may be said, however, that the phenomenon remains far from being understood. The nucleate boiling is a kind of problem non-reproducible in character. The non-reproducible character consists in creation of bubble nuclei. As the bubble nuclei are created in very fine irregular cavities on heating surfaces, their creation can not be treated from

macroscopic point of view, and there is no alternative but to treat it as phenomenon governed by chances. If we put the creation of bubble nuclei out of consideration, the phenomenon taking place thereafter growing and rising of bubbles will not have the non-reproducible character any longer and can be treated by physics of continium.

The problem of nucleate boiling has been studied by many investigators from the following two aspects:

a) Fluid Flow Problem.

b) Heat Transfer Problem.

1.3(a) Fluid Flow Problem

As in any other convective process the heat transfer to a boiling liquid depends up on the flow conditions of the fluid. An understanding of the flow and of the flow regimes is therefore a pre-requisite for an analysis of the process of heat transfer. In nucleate boiling this entails an understanding of the processes associated with the vapour generation (nucleation and bubble growth) and with the problem of vapour removal.

1.3(b) Bubble Growth: Source Flow.

Following the nucleation from a cavity, the bubble grows in superheated liquid film adjacent to the heating surface. The bubble growth has been predicted by Fritz and Endo by the equation of the form,

$$D = \frac{4\,(T_w - T_{sat})\,C_l \rho_l}{\rho_v\, h_{fg}} \sqrt{\left(\frac{\alpha t}{\pi}\right)} \qquad 1.1$$

which approximates satisfactorily the experimental data of Staniszewski for water and methanol in pool boiling at saturation temperature. Since local conditions in pool boiling are neither known nor measured, therefore, the average value of $(T_w - T_{sat})$ can predict only the average growth and not the growth of a specific bubble (unless it coincides with the average one).

Although the bubble slightly deforms (it flattens) while growing attached to the surface. Conceptual models based on the source flow (Fig.1.3) were formulated by Bankoff for nucleate boiling of subcooled liquids and by Zubor[3] for liquids at saturation. The fig. 1.3 gives a schematic representation of source flow and the wake flow associated with growing and departing bubbles.

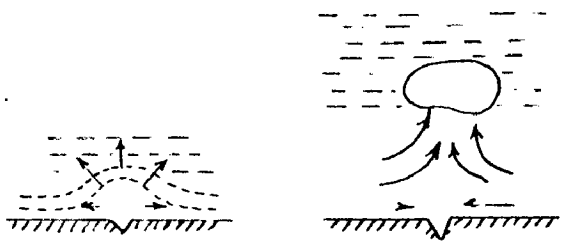

FIG. 1.3 A SCHEMATIC REPRESENTATION OF THE SOURCE FLOW AND OF THE WAKE FLOW ASSOCIATED WITH THE GROWING AND DEPARTING BUBBLE.

1.3.c Departure of a bubble: The Wake Flow.

A bubble grows and remains attached to the surface until, at time t_b (where t_b is bubble break-off time) it reaches a characteristic diameter D_b(where D_b is the diameter of break-off bubble) breaks off and departs from the heating surface. The departure is governed by the dynamics of surrounding liquid as well as

by buoyant and adhesion forces. Fritz considered only the static equilibrium between buoyant and adhesive forces, and derived the following equation,

$$D_b = C_d \beta \left[\frac{g_o \sigma}{g(\rho_L - \rho_V)}\right]^{\frac{1}{2}} \qquad 1.2$$

where

C_d = constant and was found to be 0.0140 for bubbles of H_2O.

Immediately after the detachment the lower surface of the bubble re-enters and deforms the bubble in the lenticular shape. Liquid is entrained in the wake of detaching and rising spherodial bubble. Consequently the flow associated with bubble departure can be approximated as wake flow (Fig. 1.3). The velocity of the rise of a spherodial bubble is given by,

$$U_t = \text{Const} \left[\frac{\sigma g (\rho_L - \rho_V)}{\rho_L^2}\right]^{\frac{1}{4}} \qquad 1.3$$

where, the value of constant has been found to be between 1.18 and 1.53. Following the departure of a bubble, colder liquid comes in contact with the solid and gets heated during a "delay time" t_d, at the end of which another bubble is nucleated from the same cavity. The new bubble grows until at time t_b, it in turn departs from the surface and process is repeated. A bubble column is thus formed by bubbles successively rising from a nucleating centre. The duration of delay time t_d depends upon the conditions in the vicinity of the nucleating cavity, i.e. up on the local heating rate, thermal fluctuations in the liquid and

the radius of the cavity. The duration of "break-off time" t_b depends on the local superheat temperature difference and on the local hydrodynamic conditions. For a given cavity, both t_d and t_b vary from run to run and varies from different cavities as well. Consequently the frequency of bubble emission is also a statistical distribution

$$f = \frac{1}{\tau} = \frac{1}{t_d + t_b} \qquad 1.4$$

Although both D_b and f are given by statistical distribution , Jakob found that their product remains constant i.e.,

$$D_b f = \text{const} \qquad 1.4a$$

1.3 d <u>The Regimes of Bubble Removal.</u>

The regimes of bubble removal in nucleate boiling from a horizontal surface were investigated experimentally by Yamagata and Nishikawa . It was also noted and discussed by Zuber, that removal of bubbles and the flow regimes described by Yamagata and Nishikawa[4] are identical with those reported by Davidson and Amick[5] , for the formation of gas bubbles at orifices.

At very low gas (vapour) flow rates the bubble formation is a problem of hydrostatics. The diameter of a bubble can be determined by considering a balance of buoyant and adhesion forces at the orifice (at nucleating centre).

Thus approximately smaller bubbles are spherical, the larger ones are spheroidal or bell type (Fig.1.4 a,b). Bubbles rise at constant velocity without interacting each other. The bubble volume is independent of vapour flow rate, but the frequency of bubble emission increases with increasing flow rate. In the literature this flow regime is referred to as "laminar" or as the region of isolated bubbles.

At intermediate vapour flow rates, the frequency of bubble formation remains essentially constant, while the b..bble volume increases with flow rate. The spacing between rising bubble decreases so that a bubble interact with its predecessor above the orifice. Coalescence takes place at the orifice. Bubbles are of uniform size and have been described as "mushroom like". In the literature this regime has been referred to as "turbulent" or the region of "multiple bubbles".

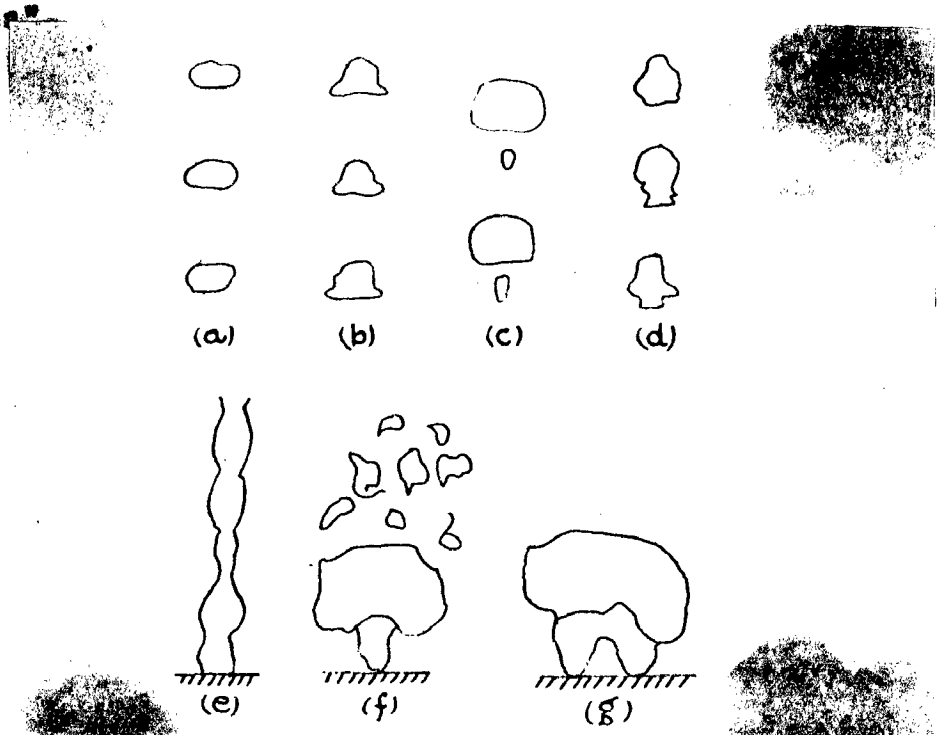

FIG. 1.4 A SCHEMATIC REPRESENTATION OF THE VARIOUS BUBBLE SHAPES IN NUCLEATE BOILING.

At still higher gas flow rates a swirling vapour stream is generated at the orifice. The jet of vapour is found to be similar to a tornado or a water spout. Large discontinuous jets are shattered into small bubbles in above orifice. (Fig. 1.4 e,f).

In nucleate boiling a bubble can interact not only with its predecessor rising above the nucleating site but it can interact with the neighbouring bubbles on the surface. Similarly two or more swirling continuous vapour columns can interact with each other. An interaction between two nucleating sites is shown in Fig. 1.4 g.

The considerations in the above lead to the conclusion that flow regimes of vapour removal from a single nucleating centre change with increasing rates of vapour generation.

1.3 (c) <u>The Flow Regimes induced by a Swarm of bubbles:</u>

In order to analyse the flow induced by a swarm of rising bubbles in nucleate pool boiling, it is advantageous to consider the similarity between nucleate pool boiling from a horizontal surface and the process of gas bubbling through a porous plate. This similarity was analysed by Zuber[3]. It was shown that both the requirement for initiating the bubbling process and the flow regimes in these phenomenon are similar. Consequently the information which is available in the literature on the hydrodynamic conditions during the

process of bubbling from a porous plate can be used to analyse the process of bubbling in nucleate pool boiling.

From experiments performed with air bubbling from perforated plates Siemes concluded that as long as spacing between active bubbling centers was greater than the diameter of bubble at departure, then the regimes of bubble removal were similar to those observed with single orifices. The experimental investigations indicate that the process of gas bubbling from porous plate is characterised by three distinct flow regimes namely "Laminar" ,"turbulent" and oscillating "slug" or "plug" flow.

The laminar flow regimes exists at low gas flow rates. Bubbles of constant volume rise without interacting with each other. This regime corresponds to the laminar regime in bubbling from an orifice. In laminar regime the liquid ahead and behind the rising bubble is at rest. No gross liquid circulation exists in the field. At these flow rates an increase of gas flow results mostly in an increase of number of active pores i.e. of bubble population.

The "turbulent" regime is characterised by the large liquid convection currents induced by rising bubbles. It can exist at low gas flow rates if the liquid is set in motion by displacement and entrainment in the wakes of rising bubbles It always exists at higher flow rates. In this regime an increase in gas flow rate results in increasing both, the bubble population and bubble volumes. Bubbles in this

region are of the "multiple types".

The change from laminar to turbulent regime is associated with bubble coalescence. In both the regimes the geometry of the vapour phase is more or less spherical. At higher gas flow rates bubbles interact and form swirling vapour columns which in turn can interact to form large vapour slugs. At those high gas flow rates the geometry of vapour phase in the vicinity of plate is columnar.

1.6 Heat Transfer Problem.

During the growth and the departure a bubble displaces liquid and entrains liquid in its wake. The flow oscillations induce large temperature oscillations in the fluid film adjacent to the heating surface and in the surface itself. The heat transfer rates in nucleate boiling were therefore attributed to the investigations of Jakob and co-workers to these bubble induced flows. It is of interest to quote the description of the flow and of the heat transfer process.

> "Strong forward and backward flows must occur in the vicinity of a growing and departing bubble. It is even possible that in between neighbouring bubble columns downward flowing streams impinge on the surface where by the heat transfer rates becomes very high ...."

> "When the vapour bubbles rise in large numbers the forced convections induced by the vaporization process becomes important "...." when bubble columns become numerous and evenly distributed

over the surface it appears visually that a liquid circulation is formed whereby liquid rises together with the vapour bubbles; flows downward at other places and flows essentially horizontally over the heating surface". " If the total heat transferred is considered as the sum of such total transfers then the heat transfer coefficient should be independent of the experimental surface.

By comparing Jakob's description of nucleate pool boiling from a horizontal surface and Townsend's description of flow regime in turbulent natural convection, it appears that flow regimes in these two heat transfer processes are rather similar. The flow through the 'conduction layer', the flow through the "up draught" , the localised nature and the maintenance of "updraught sites" described by Townsend are similar to the flow parallel to the surface and to the flow associated with a bubble column rising above a nucleating site as described by Jakob. The flow depicted in Fig.1.3 can be looked upon as "updraught" induced by the bubble motion. The temperature fluctuations in the regions of "activity" described by Townsend, and which are characteristics of convective processes arising near the boundary are not dissimilar with temp. fluctuations observed in the nucleate boiling in the vicinity of heating surface.

In view of the foregoing it appears desirable to formulate heat transfer problem by considering turbulent natural convection.

1.5 FACTORS AFFECTING NUCLEATE POOL BOILING.

(a) Pressure-

In boiling liquid, pressure affects the rate of growth of a bubble and therefore affects the temperature difference between the heating surface and the bulk liquid. Experiments performed by Farber and Scorah[1] for water boiling at different pressures show that the temperature difference decreases for a given heat flux as the pressure increases. It has also been shown that the maximum allowable heat flux for boiling liquid increases with pressure till the critical pressure is reached, and henceforth decreases with pressure. The fig. 1.5 shows the effect of pressure on boiling.

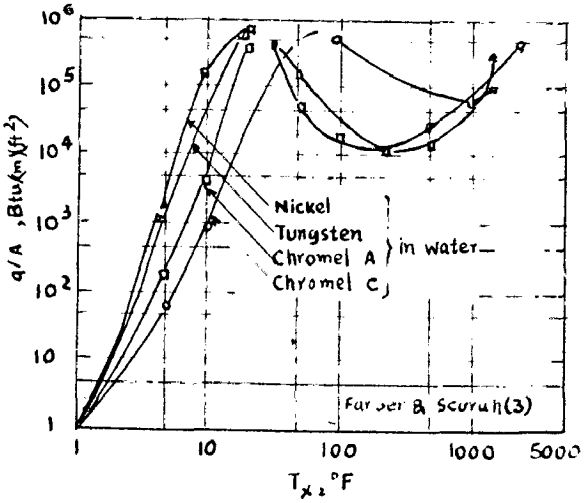

FIG.1.5 EFFECT OF SURFACE MATERIAL ON BOILING.

(b) Material of the Heating Surface.

The effect of material of the heating surface on the boiling film coefficient of heat transfer has been studied by McAdams[2] and others. At a given pressure, for a given temperature difference, between the surface and the boiling liquid, the convective film coefficient is definitely

higher for some material than the others. In order to observe this phenomenon more clearly and to obtain detailed quantitative results, H_{su}[6] conducted a series of experiments using different materials on the surface of black steel wires. The curves of film coefficient h versus the temperature difference ΔT_x are shown in Fig. 1.6.

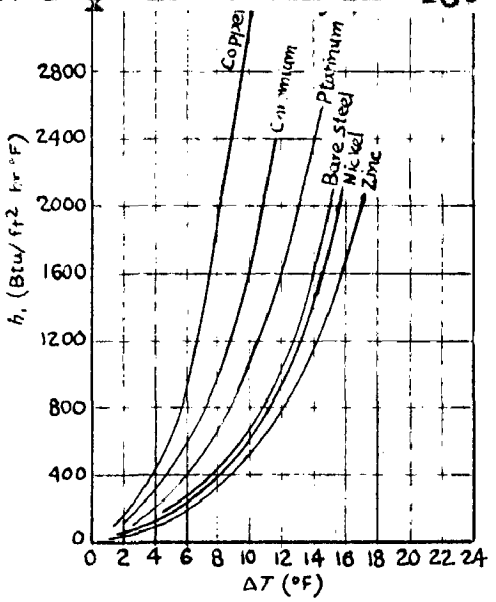

FIG. 1.6 BOILING FILM COEFFICIENT VS TEMP. DIFFERENCE FOR VARIOUS MATERIALS OF HEATING SURFACE

(c) Presence of Gas and Nature of Surface.

Head and others investigated the effect of presence of dissolved gases. As a result of this work it was concluded that dissolved gas had little effect on the attainable liquid superheat, but gas dispersed in small bubbles or entraped in surface gas pockets lowered the degree of superheat attainable This might indicate that gas bubble with a relatively large radius of curvature causes nucleation at the small amount of superheat.

When a bubble has formed, a set of interfacial

forces are set up as shown in Fig. 1.7, with a lateral

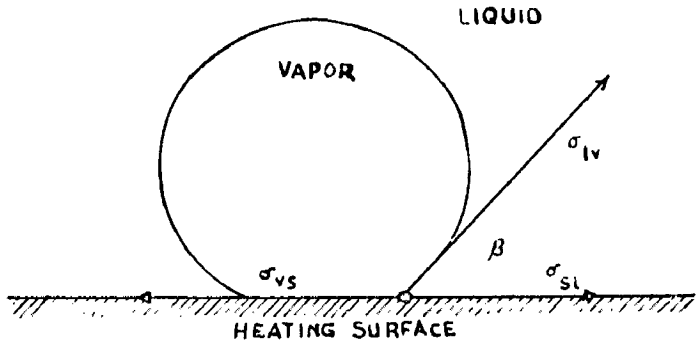

FIG.1.7 SURFACE TENSION FORCES ACTING AT POINT BUBBLE CONTACT.

equilibrium balance in the form of

$$\sigma_{vs} - \sigma_{sl} = \sigma_{lv} \cos \beta$$

The term $(\sigma_{vs} - \sigma_{sl})$ is called adhesion-free energy and determines the angle β. If its value is positive, β is less than 90^0 and the liquid is said to wet the surface. Larson suggests that for $\beta = 90^0$ bubble formation should occur without liquid superheat, that for $\beta < 90^0$ (Fig. 1.8a) bubble formation can not occur without some liquid superheat and that for $\beta > 90^0$ (Fig. 1.8c) a very thin vapour film should form on the surface at a temperature less than the normal boiling temperature. If the gas is absorbed or adsorbed on the surface, or if a gas is liberated because of a chemical process, bubble formation might occur below the normal boiling point, the bubble containing both vapour and gas. Fig. 1.8 shows the effect of interfacial tension on the shape of bubbles i.e. the angle of contact between the bubble and the heating surface, which is a measure of wettability of a surface with a particular fluid. The Figs. 1.8 shows that contact angle decreases with greater

wetting. A totally wetted surface has the smallest area covered by vapor at a given excess temperature and consequently represents the most favourable condition for efficient heat transfer.

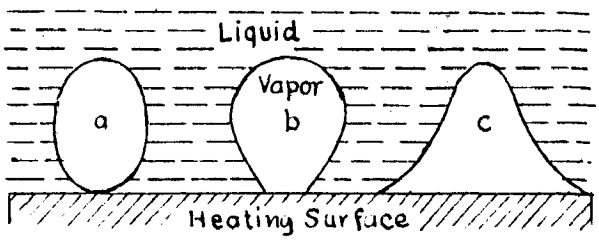

FIG. 1.8 EFFECT OF INTERFACIAL TENSION IN SHAPE OF BUBBLES.

(d) <u>Temperature of Liquid.</u>

A study was made by Cryder and Finalborgo[7] to determine the effect of liquid temperature on the boiling film coefficient. The liquids tested include water, methanol and carbon-tetrachloride. The experimental results for water are shown in Fig. 1.9.

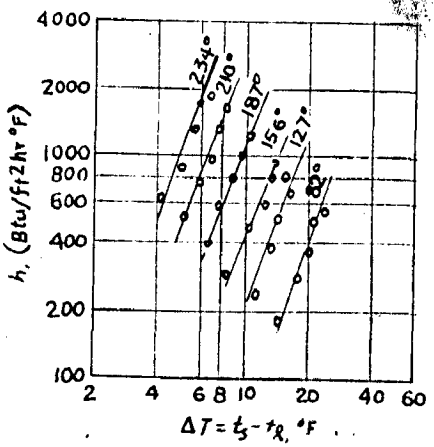

FIG. 1.9 h VS. Δt FOR BOILING LIQUIDS AT VARIOUS LIQUID TEMPERATURES.

(e) Physical Properties of the Fluid.

The data from Cryder and Finalbargo for the liquids tested were studied by McAdams and plotted in a graph of boiling film coefficient versus temperature difference, as shown in Fig. 1.10. Under the same conditions different liquids give different values boiling film coefficient. In general bubble size increases with the dynamic viscosity of the liquid. As bubble size increases the frequency of bubble formation decreases. This reduces the rate of heat transfer.

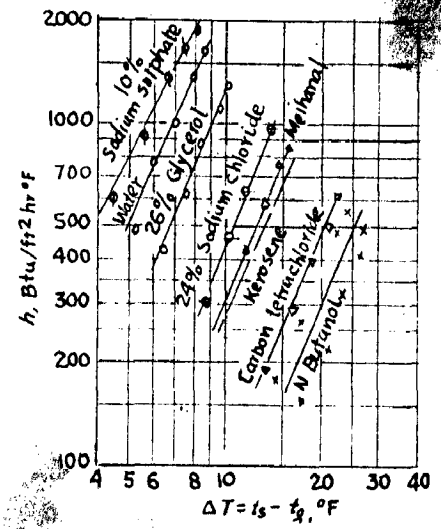

FIG. 1.10. h VS. Δt FOR VARIOUS BOILING LIQUIDS.

(f) Mechanical Agitation.

The effect of agitation on a boiling liquid was investigated by Pramuk and Westwater. Methanol was boiled under atmospheric pressure. The agitation was carried out by means of a propeller at speed upto 1000 r.p.m. The heater was a steam heated horizontal copper tube. It was found

that rate of heat transfer increased as the degree of agitation increased, at any temp. difference. The results obtained shows that heat transfer may be increased more than 100% by agitation.

CHAPTER 2

HEAT TRANSFER DURING EVAPORATION

A method of correlating the heat transfer data in nucleate pool boiling in the form of general equation for forced convection has been dealt. The correlation application to the experimental data of various investigators has also been dealt. Finally the heat transfer in boiling with forced convection is discussed.

NOMENCLATURE

A	Total heat transfer area ft^2.
A	First term in equation for surface tension lbf/ft.
B	Coefficient for ^{o}F in equation for surface tension lbf/ft.^{o}F.
C	Coefficient for F^2 in equation for surface tension lbf/ft.F^2.
D_b	Diameter of the bubble as it leaves the heating surface.
E'	Initial internal energy of vapour bubble, Btu.
E''	Final internal energy of vapour in bubble.
E_f	Internal energy of film.
e	Unit internal energy of liquid Btu/lb.
f	Surface area of bubble (ft^2)
f	Frequency of bubble formation.
G_b	Mass velocity of bubbles at their departure from heating surface.
g	acceleration of gravity.
g_c	Conversion factor.
h_{fg}	Latent heat of evaporation Btu/lb.

h^*	Unit enthalpy of vapour in bubbles Btu/lb.
h_L	Unit enthalpy of liquid Btu/lb.
K_L	Thermal conductivity of liquid (Btu/ft.hr.^oF)
n	Number of bubbles per unit surface .
N_u	Nusselt Number.
N_{pr}	Prandtl Number.
Mo	Initial mass of vapour in bubble (lbm)
M	Mass of vapour in bubble.
dm	Incremental mass of liquid.
mf	Mass of matter in film.
p_L	Liquid pressure lbf/ft^2.
p^*	Vapour pressure lbf/ft^2.
Q	Heat quantity.
r'	Initial bubble radius ft.
r*	Final bubble radius ft.
T	Abs tem. ^oR
ΔTx	Temp. differential between tube surface and saturation temp ^oF.
u'	Initial unit internal energy of vapour in bubble Btu/lb.

u''	Final unit internal energy of vapour in bubble Btu/lb.
u_L	Unit internal energy of liquid.
u_f	Unit internal energy of film.
V_{sys}	Volume of system Cu.ft.
v_L	Unit volume of liquid ft^3/lb.
v'	Initial volume of vapour in bubbles ft^3/lb.
v''	Final volume of vapour in bubble.
W	Work quantity Btu.
σ	Surface tension $A + BT^2 + CT^2$ lb/ft^2.
C_{sf}	Coefficient which depends on nature of fluid heating surface combination.
β	Bubble contact angle in degrees.
ρ_L	Density of saturated liquid lb/cu.ft.
ρ_v	Densityof saturated vapour lb/cu.ft.
μ_L	Viscosity of saturated liquid lbm/ft.hr.

It seems almost impossible to obtain single heat transfer co-relation equation to correlate the effects of pressure, kind of liquid, and kind of heating surface over the entire range of Δt, including all the regimes of boiling. This difficulty arises from the fact that the heat transfer mechanism differs radically in various regimes. Reasonably successful attempts have been made to correlate the data within a region where a particular regime prevails. For example, in the regime of interface evaporation where no bubbles are formed, have been correlated by ordinary natural convection equations. The data in regime of nucleate boiling have been correlated, for atleast the effect of pressure on the boiling process. The data in regime where stable film boiling occurs, have been correlated in still a third way. The transition-type regions remain un-correlated.

1.1 CORELATION OF POOL BOILING HEAT TRANSFER DATA.

Since the major portion of the heat is transferred directly from the surface to the liquid and the bubbles act as agitators, it seems desirable to look for a comparison at the heat transfer in forced convection turbulent flow without boiling. In this latter case the heat transfer data are correlated by a relation,

$$N_{NU} = \phi \ (N_{Re} , N_{Pr}) \qquad . 2.1$$

For pool boiling essentially with saturated liquids Jakob shows that the heat transfer from the surface is for the most part transferred directly to the liquid, the increased heat transfer rate associated with boiling being accounted for by the resulting agitation of the fluid by motion of the liquid flowing behind the wake of the bubble departing from the surface. Rohsenow and Clark[8,9] showed a similar result in studying motion pictures of McAdams for subcooled liquids flowing in forced convection with surface boiling but no net generation of vapour. Gunther and Kreith[10] and Gunther[11] presented photographic evidence that in highly subcooled liquids in pool boiling and in forced convection with surface boilings, the bubbles could form at the surface, grow and then collapse while remaining attached to the surface.

As the rate of heat transfer is increased and bubble agitation becomes more vigorous, the effect of forced convection fluid velocity and hence the Reynolds number based on the pipe diameter becomes less and less. This effect is shown by the data of Rohsenow and Clark[8] reproduced in Fig. 2.1. This data is representative of data of others for surface boiling with forced convection. In this figure the curves of various fluid velocities are shown to merge into one curve, showing that as the boiling becomes more vigorous, the effect of fluid velocity disappears. It seems reasonable then to seek a

correlation of heat transfer data by means of a bubble Reynolds number based on bubble dia. and velocity.

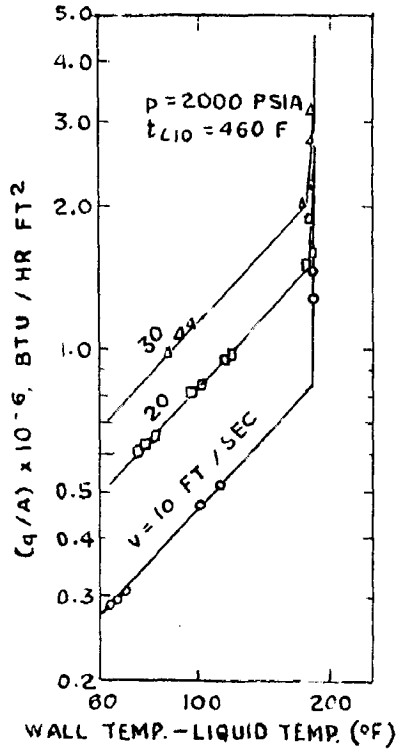

FIG. 2.1 EFFECT OF FLUID VELOCITY ON HEAT TRANSFER RATE IN NUCLEATE BOILING.

For the purpose of analysis one can visualize a number of streams of bubbles receding from the heating surface and a bubble Reynolds number defined by

$$N_{Re,b} = \frac{G_b \quad D_b}{\mu_L} \qquad 2.1$$

based on the mass velocity of the bubbles and their diameters as they leave the surface. The Reynolds number is often interpreted as a ratio of inertia to viscous forces. Hence G_b associated with the inertia of the bubble and μ_L associated with friction force on the bubble are used in equation 2.2.

Since from continuity the rate of liquid flow toward the heating surface equals the rate of vapour flow away from the surface, then $G_b = G_l$ and the inertia force of $N_{Re,b}$ may alternatively be thought to be that associated with the liquid agitation resulting from the bubble motion G_b.

Since most of the heat is transferred to the liquid as in the case of non-boiling forced convection, the Prandtl number of the liquid ought to appear in the boiling correlation, since it appears in equation 2.1. Then for pool boiling,

$$N_{Nu,b} = \phi_b \left(N_{Re,b} , N_{Pr,l}\right) \qquad 2.2$$

where,

$$N_{Nu,b} = \frac{(q/A)\, D_b}{\Delta T_x \quad K_L} \qquad 2.3$$

which is a bubble Nusselt number with $h_x = (q/A)/\Delta T_x$ Assuming that the bubbles on the average, may be approximated as spheres,

$$G_b = \frac{\pi}{6} D_b^3 \quad \rho_v \, f \, n$$

The rate of heat transfer to the bubble as it breaks of from the surface will be obtained by considering the thermodynamics of vapor bubbles.

2.1(a) Heat Transfer to Bubbles:

The formation of a single bubble is analysed by considering an incremental growth in an existing bubble and writing the corresponding heat quantity dQ, in terms of energy and work quantities, dE and dw. The resulting expression for dQ is then integrated from zero bubble radius to a finite radius giving the heat required to form a bubble of that size. During this incremental change it is permissible to define a system to include the vapour in the bubble, the liquid which is vaporized during the change, and the liquid film which constitutes the phase boundary. The phase boundary is also considered to be a control surface across which the work and heat flow. From first law, we have

$$dE = dQ - dw \qquad 2.5$$

The work quantity dw is that work done by the system on the surrounding liquid and is written,

$$dw = p_L \, dV_{sys}$$

$$= - p_L \, v_L \, dm + p_L \, dV_{bubble} \qquad 2.6$$

The change in the internal energy of the system is written

$$dE = E'' - (E' + e \, dm) + dE_f \qquad 2.7$$

Therefore, combining equations 2.6 and 2.7 it is found,

$$E'' - (E' + e\,dm) + dE_f = dQ + p_L v_L\,dm - p_L\,dV_{bubble} \quad -2.8$$

or neglecting Kinetic energy and Potential energy terms, equation 2.8 becomes

$$(M_o + dm)\,u'' - Mou' - u_L dm + dE_f - p_L v_L\,dm + p_L\left[(m_o + dm)\,v'' - Mov'\right] = dQ \quad -2.9$$

Since the change in energy of bubble is due primarily to the transfer of mass dm and is much less dependent upon the change in the thermodynamic state of vapour within the bubble due to this mass transfer, e.g. state $(\ )'' \cong$ state $(\ )'$ Equation 2.9 becomes,

$$u''\,dm - u_L\,dm - p_L v_L\,dm + p_L v''\,dm + dE_f = dQ \quad -2.10$$

and integrating this expression from $M = 0$, e.g. all liquid to $M = M$.

$$M\,(u'' - u_L - p_L v_L + p_L v'') + E_f = Q \quad -2.11$$

Now the energy of the film on the fully developed bubble may be written,

$$E_f = TS_f + \sigma F + U_f m_f$$

But since the mass of the film m_f is extremely minute,

this is written with practically no error

$$\frac{E_f}{F} = \sigma - T\left(\frac{\partial \sigma}{\partial T}\right)$$

so that Equation 2.11 is then given,

$$M\left[u^* + p_L v^* - (u_L + p_L v_L)\right] + F - FT\left(\frac{\partial \sigma}{\partial T}\right) = Q \qquad - 2.12$$

Now, the mass of the bubble is $\left(\frac{4}{3}\pi\right)\left(\frac{r^{*3}}{v^*}\right)$, its surface area is $4\pi r^{*2}$, and p_L is related to p^* through the expression for equilibrium,

$$p_L = \frac{p^* - 2\sigma}{r^*}$$

Substituting these into equation 2.12 and re-arranging, expressing $u + p_v$ as equal to h, we arrive at expression giving the heat quantity required to form a single bubble of radius r^*.

$$Q = \frac{4\pi}{3}\left\{\frac{r^{*3}}{v^*}(h^* - h_L) - 2r^{*2} + 3r^{*2}\left[\sigma - T\left(\frac{\partial \sigma}{\partial T}\right)\right]\right\} \qquad -2.13$$

The last term in the brackets accounts for the energy

change of the phase boundary during the transformation and is similar to that given by Larson. With σ given as $\sigma = A + BT + CT^2$ With 2.13 becomes,

$$Q = \frac{4}{3}\pi r^3 \left\{ \frac{r^n}{v^n} (h^n - h_L) + A - 2BT - 3CT^2 \right\} \qquad - 2.14$$

where, Q is in Btu per bubble of radius r^n.

Except for very small bubbles ($r^n < 2 \times 10^{-5}$ ft) the terms $A - 2BT - 3CT^2$ in equation 2.14 may be neglected Also the effect of curvature on equilibrium saturation conditions is important for very minute bubbles. ($r^n < 10^{-7}$ ft) so that h^n becomes h_G and h_L is that liquid enthalpy corresponding to the temperature of the superheated liquid from which the bubble forms. Equation 2.14 may be written with good approximation as

$$Q = \frac{4}{3}\pi r^{n3} \frac{hf_G}{v^n} \qquad 2.15$$

where all the properties correspond to the saturation state at the pressure of the liquid. This form of equation has also been suggested by Boonjakovic.

The rate of heat transfer to the bubbles per square foot of heating surface area is,

$$(q/A)_b = hf_G \frac{\pi}{6} D_b^3 f \rho_v n \qquad 2.16$$

where, $D_b = 2r^n$

and $\rho_v = \frac{1}{v^n}$

Since h_{fg} and ρ_v are functions of pressure, $(q/A)_b$ is a function of β, pressure and n.

Gunther[11] has shown that D_b does not change appreciably with q/A. At a given pressure, if is assumed to be independent of q/A, then $(q/A)_b \propto n$ and since $\uparrow q/A$ is also proportional to n, hence, $q/A \propto (q/A)_b$ 2.17

or from equation 2.16,

$$q/A = C_q h_{fg} \frac{\pi}{6} D_b^3 f \rho_v n, \qquad 2.18$$

where, C_q is the coefficient of proportionality.

II.1.b Non-dimensional Groups.

Expressions for $N_{Re,b}$ and $N_{Nu,b}$ are obtained by substituting equations 1.2, 2.6 and 2.16 into equations, 2.1 and 2.3

we have,

$$N_{Re,b} = C_R \beta \frac{q/A}{\mu_L h_{fg}} \sqrt{\frac{g_0 \sigma}{g(\rho_v - \rho_L)}} \qquad 2.19$$

and

$$N_{Nu,b} = C_N \beta \frac{q/A}{\Delta T_x K_L} \sqrt{\frac{g_0 \sigma}{g(\rho_v - \rho_L)}} \qquad 2.20$$

where, $C_R = \sqrt{2}\, C_d/C_q$ and $C_N = \sqrt{2}\, C_d$

Each of these expressions is dimensionless, as is β, which is in radians of an arc.

In equation 2.2 the rules of dimensionless analysis permit the replacement of $N_{Nu,b}$ by any product of powers ofother dimensionless group.

A convenient group is,

$$\frac{N_{Re,b}\ N_{pr,f}}{N_{Nu,b}} = \frac{C_f \Delta T_x}{h_{fg}} \qquad 2.21$$

which is a new dimensionless group interpreted as the ratio of liquid superheat enthalpy at the heating surface to the latent enthalpy change in evaporation.

Then equation , 2.3 may be replaced by,

$$\frac{C_f\ \Delta T_x}{h_{fg}} = \psi_b (N_{Re,b},\ N_{pr,f}) \qquad 2.222$$

II.2. Correlation Application.

The proposed correlation equation 2.22 has been applied to the data of various experimenters. It will be of interest to know the detail of its application to the data of Addoms[8], for pool boiling of water because of wide range of pressure covered. - 14.7 psia to 2465 psia. In these experiments degassed distilled water was boiled by means of an electrically heated horizontal platinum wire. Data for a wire of dia.0.026 inch are shown in Fig. 2.2. A plot of

$$\left[\frac{(q/A)}{\mu_L h_{fg}}\right]\left[\frac{\sigma g_c}{g(\rho_L - \rho_v)}\right]^{\frac{1}{2}} \quad Vs \quad \frac{C_L\ \Delta T_x}{h_{fg}}$$

is shown in Fig. 2.2b. On this plot the positions of these

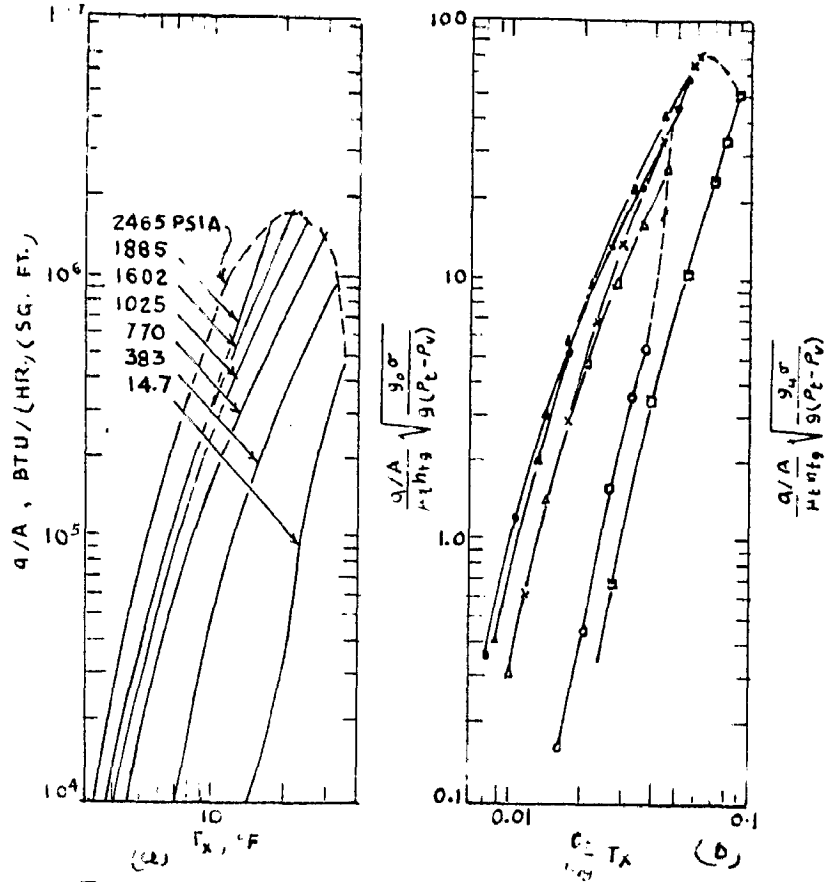

FIG. 2.1 CORRELATION OF DATA OF ADDOMS[10] FOR PLATINUM-WATER INTERFACE FOR POOL BOILING.

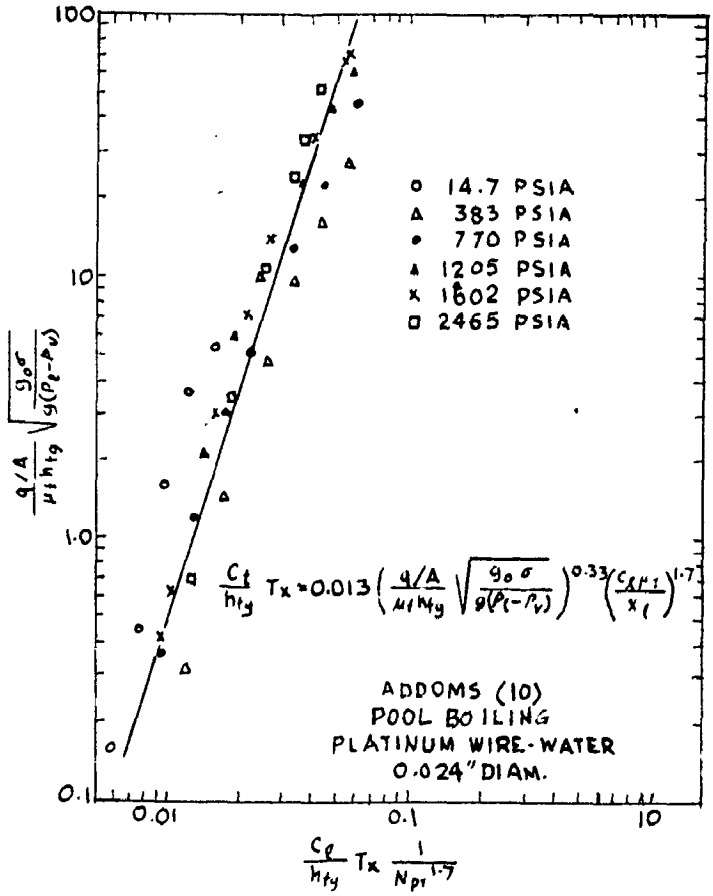

FIG 2.2 CORRELATION OF DATA OF ADDOMS[10] FOR PLATINUM-WATER INTERFACE FOR POOL BOILING.

lines rise to a maximum with pressure and then falls. At the pressure corresponding to the highest line on this spot, the prandtl is very nearly at its minimum value. If the function ψ_b of equation 2.22 is expressed as a power series and if only first term is used

$$\frac{C_\ell \Delta T_x}{h_{fg}} = C_{sf}\left[\frac{q/A}{\mu_\ell h_{fg}}\sqrt{\frac{g_0\sigma}{g(\rho_L-\rho_v)}}\right]^r\left[\frac{C_\ell \mu_L}{K_\ell}\right]^s \qquad 2.23$$

where C_{sf} = (Constant) and hence should be a function of the particular fluid heating surface combination. From Fig. 2.2a and 2.2 b the exponent r was obtained. A cross plot of $\frac{C_\ell \Delta T_x}{h_{fg}}$ Vs N_{Pr} for the constant values of ordinate gave the value of exponents. The final co-relations has been shown in Fig. 2.2c which results in C_{sf}= 0.013, with a spread of approximately ± 20%.

This process was repeated for the data of Cichelli and Bonilla and Cryder and Finalborgo giving the values of C_{sf} for various fluid-heating surfaces. Since the magnitudes β were not available for those data, therefore, β of $N_{Bo,b}$ was included in the term C_{sf}.

It has been emphasized that accurate values of fluid properties are essential in obtaining a co-relation applies only to clean surfaces.

II. Heat Transfer in Boiling with Forced Convection.

The foregoing method of corelating data for nucleate pool boiling has also been applied successfully to boiling of fluids inside tubes by forced and natural convection. Fig.2.3 shows the curve of boiling data of sub-cooled forced convection in tubes. The system in which these data were obtained consisted of a vertical annulas containing an electrically heated stainless steel tube placed centrally in tubes of various diameters. Degased distilled water was passed through the annuhas at velocities from 1 to 12 fps and pressures from 30 to 90 psia.

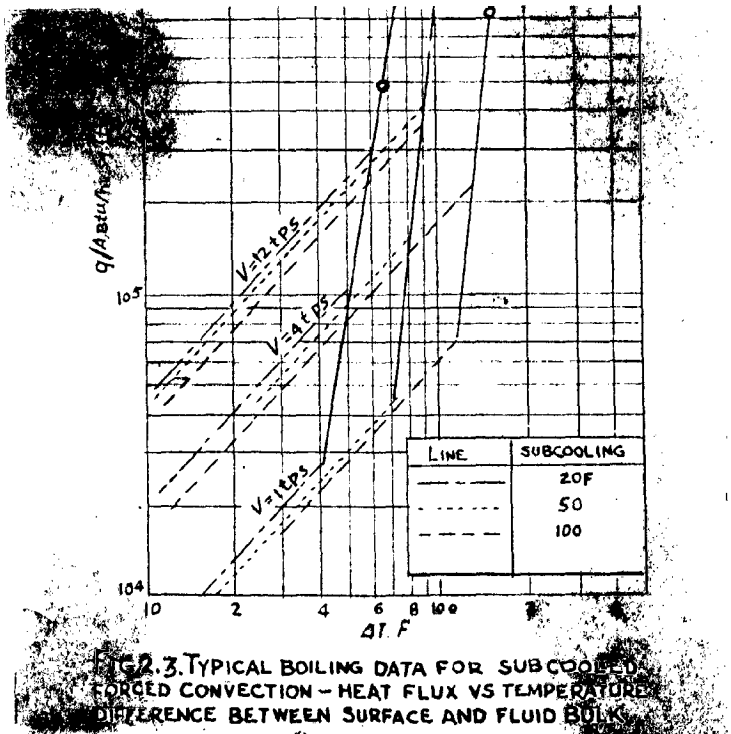

FIG 2.3. TYPICAL BOILING DATA FOR SUBCOOLED FORCED CONVECTION – HEAT FLUX VS TEMPERATURE DIFFERENCE BETWEEN SURFACE AND FLUID BULK.

The dotted lines represent forced convection conditions at various velocities and various degrees of subcooling. The solid lines show the deviation from forced convection caused by surface boiling. The beginning of boiling caused

$$St = \phi\ (N_{Re})\ \psi\ (N_{pr})\ (\mu_b/\mu_s)^n$$

This value of q_b is then used in equation 2.24 in the same manner as total heat flux in nucleate pool boiling.

by increasing the heat flux depends upon the velocity of the fluid, and the degree of subcooling below its saturation temperature at the existing pressure. An increase in the velocity increases the effectiveness of forced convection, decreases the surface temperature at a given heat flux and thereby delays the onset of boiling. In the boiling region the curves are steep and the wall temperature is practically independent of fluid velocity. This shows that the agitation caused by the bubbles is much more effective than the turbulence in forced convection without boiling.

To apply the pool boiling corelation to forced-convection boiling, the total heat flux must be separated in two parts one a boiling heat flux q_b/A, the other convective heat flux q_c/A, or

$$q_{Total} = q_b + q_c$$

The boiling heat flux is determined by subtracting the heat-flow rate, accountable for by forced convection alone, from the total heat flux, or

$$q_b = q_{Total} - A \bar{h}_c^{\,\prime\prime\prime} (T_s - T_b) \qquad 2.24$$

where h_c is determined from the equation of the type

$$St = \phi\ (N_{Re})\ \psi\ (N_{pr})\ (\mu_b/\mu_s)^n$$

This value of q_b is then used in equation 2.24 in the same manner as total heat flux in nucleate pool boiling.

CHAPTER III

VAPORIZATION INSIDE HORIZONTAL TUBES

The flow patterns for two-phase flow have been discussed as studied by different investigators. A brief literature survey is then made of the experiments conducted by various experimenters to determine the heat transfer rates of evaporating refrigerants in tubes. Finally the co-relation equations given by B.Pierre have been discussed.

Vaporization of refrigerants inside horizontal tube has been studied theoretically and experimentally by many researchers. It will be of a particular interest to know the flow mechanisms in evaporator tubes. Since both liquid and gaseous phases of refrigerant are present in all parts of evaporator, we are dealing with two phase flow the kinetics of which are more complicated than those of single phase flow. The various forms of two phase flow provides us with further possibilities to evaluate and to improve the heat transfer processes in an evaporator.

Flow Patterns in Two phase Flow.

The most thorough investigations of two phase flow were made with air water and air-oil systems. Hoogendoon whose investigations of two-phase systems at the Royal Shell Laboratory in Amsterdam were confirmed by others, discovered the following seven distinct possibilities for two phase flowing beside each other. They are illustrated in Fig. 3.1.

(1) Both phases are calmly flowing by the side of each other separated by a plane surface.

(2) Both phases are separated by a wavy surface.

(3) The gaseous phase above the wavy separation surface contains a part of the liquid phase in the drop form.

(4) Slugs of liquid are enclosed in the gas stream and travel with flow gas stream.

(5) The waves of separation surface between the phases are turbulent.

(6) Liquid flows preferentially in an annular pattern along the tube-wall, while the gas forms a flow nucleus within this cylinder which contains a part of the liquid phase in the drop form.

(7) The gas and liquid are flowing through the tube as a foam.

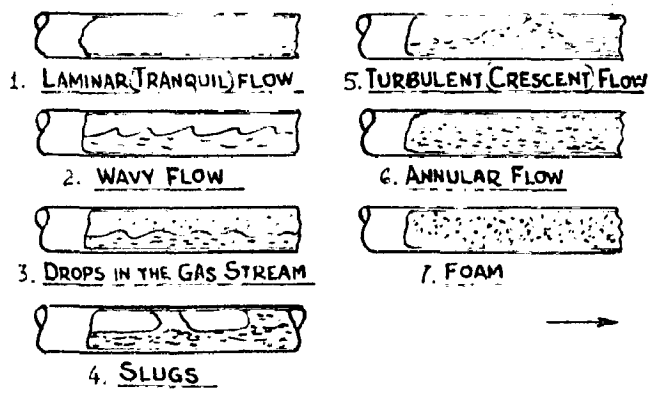

FIG.3.1. FLOW PATTERNS

The flow pattern enumerated here correspond to definite mass flow rates of each phase and occur at definite gas and liquid velocities. The flow pattern described here were also observed in the streams of boiling refrigerant

(B_{11} and B_{12}) depending upon the heat flux density as well as vapour velocity. Findings by Bryan and Seigel[12] latter confirmed by Baker[13] indicate that a laminar flow pattern with little wetting occurs at low rates of heat flux density, changing to a wavy pattern towards the evaporator outlet. At high heat flux ranging from 1950 to 3700 Btu/hr sq.ft, slug shaped or ring shaped flow was observed beginning at the evaporator inlet. Worsoe and Schmidt[15] confirmed these results from observations on a refrigerant$_{-12}$ glass evaporator which enabled him to determine the flow patterns of fig.3.1 occur in the sequence as either gas velocity or heat flux density increases. Recent investigations by Hufschmidt also indicate a definite separation of liquid and gas flow rates of heat flux density (as for instance in air-cooling units) and that no foaming takes place.

At the same time, Hufschmidt expressed the conjecture that in the case of laminar flow, refrigerant occurs in the form of a thin film in areas which are not wetted by liquid. According to observations by Worsoe-Schmidt, this is the case only if oil is present. Baker also indicates that non-wetted surface participate in heat trqnsfer process to only a small extent, as hqt heat transfer coefficient in such areas are very low.

Measurements by Davis and investigations by Murray[16] support the concept that the heat transfer depends to a large extent on the wetting of the tube wall which in turn depends on the flow pattern. This statement is essentially in agreement

with Pierre equation according to which heat transfer coefficient increases with increase of refrigerant flow rate.

Literature Survey.

Various experimental investigations have been made for studying the heat transfer characteristics of evaporating refrigerants in tubes. The evaporator heat transfer analysis was initiated by Frank O.Gaskill[17] in 1933. The latest contribution towards this field known to author is by Katiani and Agaliani[18] Dec. 1963. The preliminary work was carried out by Martin[19] 1930, McAdams, Woods and Bryan[20] 1941, Ashley[21] 1942, and Witzig, Penney and Cyphers[22] in 1948. The progress was further made by Frank 1951, Yoder and Dodge[24] 1952, Baker, Touloukian and Hawkins[26] 1953, De-Pierre 1954, Bryan and Siegel 1955, Baker 1956, Hoffman 1957, Murray 1959, Altman, Norris and Staub[27] 1960 and R.Folks[28] 1963.

Ashley[21] in 1942 made tests to determine the heat transfer of evaporating $Freon_{-12}$ in a 0.575" I.D. Copper tube. The test evaporator worked on mechanical vapour compression system. Load, flashing gas, suction temperature and the amount of excess liquid were varied. An analysis of the results indicated that the $Freon_{-12}$ heat transfer may be correlated with mean load on the evaporator (including flash gas). It was believed that the variables of diameter, length of circuit and method of circuiting may be included to express a general relationship.

Uitzig, Penny$_2$ and Cyphers[21] in 1948 performed experiments to determine heat transfer rates of evaporating Freon$_{-12}$ in a horizontal 0.305 inch I.D. Copper tube. The effects of mass flow rate, progressive evaporation, evaporation temperature and oil contamination were studied. In their test set-up compressor was not used in the circulating system. The first tests were to employ oil-free Freon, and then the tests were followed in which oil was added in definite amounts. It was found that for lower mass flow rate range (upto 16 lbs/hr) it had no effect on the temperature difference between tube and evaporating Freon. At the highest rates of power input, the mass flow rate also had little effect. A statistical treatment of the data confirmed this. While examining the temperature distribution along the evaporator tube, it was found that under conditions, where a high percentage of Freon was being evaporated, a sharp rise in the temperature was observed until this point is reached, the temperature of the evaporator is constant. This again holds good for a lower mass flow rate. However, this has not been observed either in practice or by other investigators.

During the study of the effect of temperature difference on the heat transfer rate, the evaporation temperature was kept constant and the results were correlated by the following equations

$$q/A = 14.3 \quad t^{2.18} \quad (4.8\,F < t < 12.8^{0}F)$$

at temperature of 68°F

$$\frac{q}{A} = 6.0 \quad t^{2.29} \quad (\ 8^{\circ}F < t < 21.7^{\circ}F\ )$$

at temperature of 19.4°F.

The effect of evaporating temperature on heat transfer rates was seen to be predominant. The heat transfer rates decreased with evaporating temperature for a constant temperature difference.

To study the effect of oil contamination 1% of oil by volume was added. The results indicated that it reduced the heat transfer rate at the given temperature difference. However, the heat transfer rate has the same functional dependence, on t as was found before.

Yoder and Dodge[24] in 1952 studied the film heat transfer coefficients for Freon$_{-12}$ boiling in the range of -60°F to -100°F. The evaporator used was vertical electrically heated tube 8 ft. long and 0.054 inch ID. The system used was 3 stage vapour compression. Results indicated that at a given heat flux density the effect of flow rate on the average boiling film coefficient was very high. It was found that one of the most important variables affecting the film coefficient was percentage vapour in the mixture.

Baker, Touloukian and Hawkins[26] in 1953

investigated the boiling of Freon$_{-12}$ for surface to bulk temperature differentials less than 12°F and flow rates less than 120 lbs. per hour. The evaporator was 0.545 inch horizontal copper tube 38" long. The heat was supplied by enveloping bath of condensing Freon$_{-11}$ vapour. The experimental results were co-related by a non-dimensionless equation of the form of Nusselt's equation.

Bryan and Seigal[12] in 1955 investigated the heat transfer coefficient of Freon$_{-11}$ in a horizontal tube. The photographic study of the mechanism by which heat is transferred was made. An analytical study of local film coefficient along the length of evaporator was also conducted. The effect of turbulance promoters was studied by introducing spiral wires inside the tubes. It was noted that the heat transfer coefficient increased with increased turbulance. The whole system was designed to work on a forced circulation system by employing a liquid refrigerant pump. The results of the test indicated that at low flow and low heat transfer rates the liquid flows at the bottom of the tube and is separated from the gas at the top by a gas liquid interface which is at times unstable. The higher gas velocity causes waves to form in the liquid at the gas liquid interface. These waves become more pronounced as the gas velocity increases until the gas under-cuts the wave and sprays the liquid on the top surface of the tube resulting in a higher heat transfer rate for the top of the tube than at the bottom. A theoretical analysis of

the flow has not been obtained and the experimental analysis presented in this investigation does not satisfactorily predict the heat transfer in bare tubes for the transition zone or when the liquid waves are picked up and sprayed in varying amount on the top surface of the tube.

Altman, Norris and Staub[27] in 1960 conducted tests to investigate local heat transfer and pressure drop of Freon$_{-22}$ evaporating in horizontal tube. The Martinelli-Nelson method of calculating two phase pressure drop inside pipes was extended for use with Freon$_{-22}$ and was then employed to correlate the pressure-drop data in this investigation.

The correlations of heat transfer for evaporating refrigerants of widest established scope seem to be the two developed by B.Pierre[35]. These corelations apply to several different refrigerants namely, Refrigerant$_{-11,12}$ and $_{22}$ and to $CH_3\,Cl$, are summarized below.( )

Equation 3.1 holds for outlet vapour qualities well below 90% dry and equation 3.2 is for complete evaporation where outlet conditions are 11°F superheat.

$$h_{ave}\,D/K_L = 0.0009 \left[\left(\frac{GD}{\mu_L} \right)^2 \left(\frac{J\,\Delta x\,\lambda}{L} \right) \right]^{0.5} \qquad 3.1$$

$$\text{for} \quad 10^9 < N_{Re}^2\, K_f < 0.7 \times 10^{12}$$

$$h_{ave}\,D/K = 0.0082 \left[\left(GD/\mu_L \right)^2 \left(\frac{J\,\Delta x\,\lambda}{L} \right) \right]^{0.4} \qquad 3.2$$

$$\text{for} \quad 10^9 < N_{Re}^2\, K_f < 0.7 \times 10^{12}$$

Where Δx = Vapour quality change
λ = Latent heat of vaporization
K_L = Load factor = $J\,\Delta x\,\lambda$
k_L = Thermal Conductivity of liquid
μ_L = Dynamic viscosity of Liquid

The major objection to Pierre's corelations is that they consider only the average, and not the local, heat transfer coefficient and that the outlet conditions are either at 11°F superheat or well below 90 percent vapour quality. The nature of any dependence of the heat transfer on local quality is therefore not considered in the Pierre's work.

CHAPTER 4

EXPERIMENTAL SET-UP AND TEST PROCEDURE.

The various points to be studied during the experimental work have been discussed. Then the choice of particular test set-up and its design has been made. The instrumentation and the test procedure has been discussed in the end.

4.1 AIM OF EXPERIMENTAL WORK.

The experimental work presented in this chapter aims at studying the following aspects of evaporating Freon$_{-12}$ in the horizontal tube.

(1) Heat transfer characteristics in the form of an equation given by Rohsenow for pool boiling.

(2) Effect of temperature difference between the tube surface and evaporating Freon$_{-12}$ on the heat transfer rates.

(3) Effect of pressure of vaporization on the heat transfer coefficient.

(4) Pressure drop as related to the heat transfer coefficient rates.

(5) Distribution of local heat transfer coefficient along the evaporator tube length.

(6) Effect of mass flow rate on pressure drop.

As already mentioned in the beginning, the variation of tube angle with horizontal may affect the heat transfer rates, therefore, the experimental work also covers the study of heat-transfer coefficients in case of inclined tube.

4.2 REQUIREMENTS OF APPARATUS:

Keeping in view the above aims, the test set-up was designed and fabricated to meet the following requirements.

(1) A closed system in which Freon$_{-12}$ passing through test section could be evaporated by the application of uniform heat flux.

(2) Varying flow rates through test section.

(3) Varying states of refrigerant entering the evaporator.

(4) Condensing the refrigerant evaporated from the evaporator test section.

(5) Elimination of oil contamination with the refrigerant.

(6) Measurement of pressure drop during evaporation at the two ends of the test section.

(7) Provision for varying the evaporator tube angle.

The vapour compression system was not employed in the test set up firstly as it would not have been possible to get oil free refrigerant and secondly pressure-pulsations would have made it difficult to measure the pressure drop. Due to non-availability of the liquid refrigerant pump, the thermo-syphon system for circulating

the refrigerant was made use of.

4.3 ASSUMPTIONS MADE IN DESIGN OF APPARATUS.

The following were the assumptions made in designing the apparatus:

1) Test Section- straight copper tube 3.5 ft. long, 3/8 inch I.D.

2) Maximum pressure drop in the whole system 5 psia.

3) Maximum saturation temperature 90°F.

4) Overall heat transfer coefficient during condensation of $Freon_{-12}$ 200 Btu/hr ft^2 F°.

5) L.M.T.D. during condensation of $Freon_{-12}$ by chilled water 12°F.

6) Maximum flow rate 3 lbs/minute.

4.4 DESIGN OF APPARATUS.

Position of Condenser:

To achieve the flow due to difference of densities of liquid and vapour column, the condenser position was determined with respect to evaporator, using difference of densities 77.6 lbs/cu.f.t.

$$\text{Height of condenser above the evaporator tube} = \frac{5 \times 144}{77.6} = 9.28 \text{ ft} \approx 10 \text{ ft.}$$

Size of Condenser.

For the sake of simplicity the condenser designed

was of shell and coil type.

Maximum heat rejection in condenser (Btu/hr) when evaporation occurs at 90°F

= (Enthalpy increase in evaporator/lb of refrigerant) x (weight of refrigerant flowing per hour) + Heat addition before and after evaporation.

= (58 x 3 x 60) + 10% of heat addition.

= (58 x 3 x 60) x 1.1

= 11,484 Btu/hr.

Heat transfer area = $\frac{11484}{12 \times 200}$

= 4.78 sq.ft. ≈ 5 sq.ft.

Taking copper tubing of ½" O.D.

Length of tube = $\frac{5 \times 24}{}$

= 38.2 ft.

Figure 4.1 shows the condenser which consists of 40 ft. long ½" O.D. Copper tube bent in form of coil enclosed in a cylindorical vessel 2' x 1'-9" prepared out of 1/16" G.I. Sheet. The coil was formed in a way as to keep constant slope downwards. The shape was maintained by providing three wooden clamps.

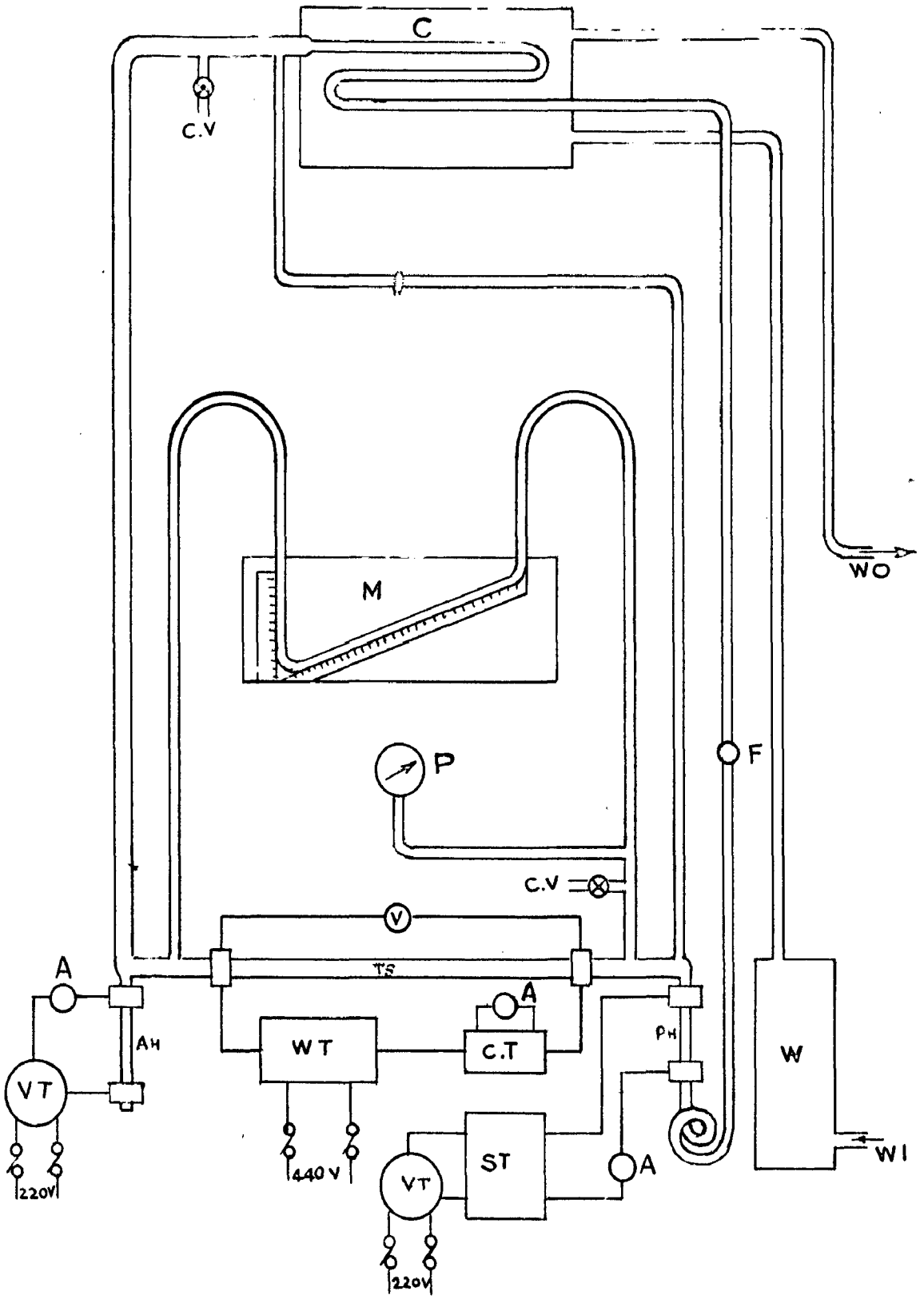

FIG 4.4 SCHEMATIC DIAGRAM OF TEST SET-UP

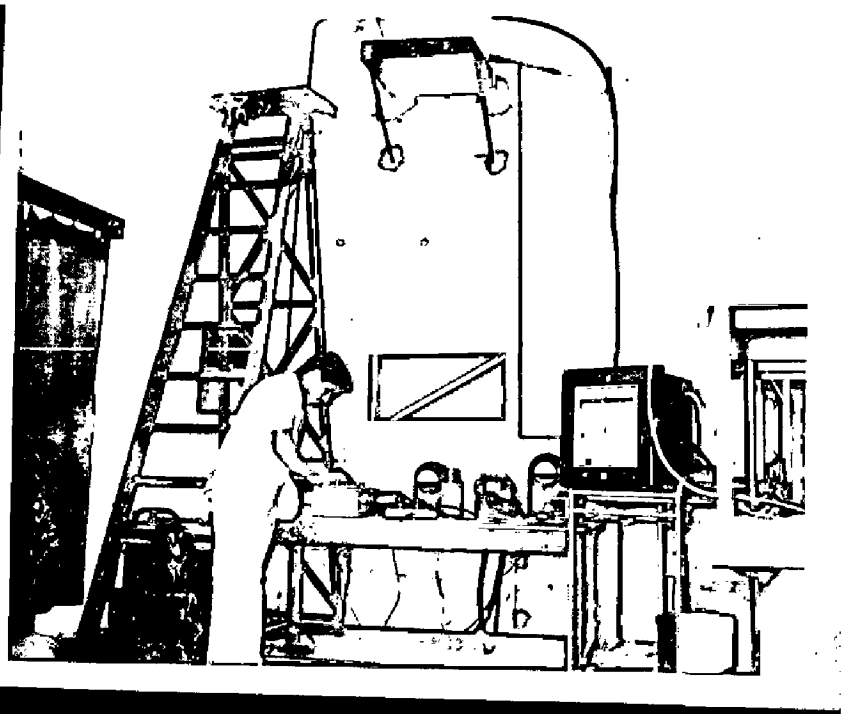

Fig. 4(i) A complete view of Test Set-up.

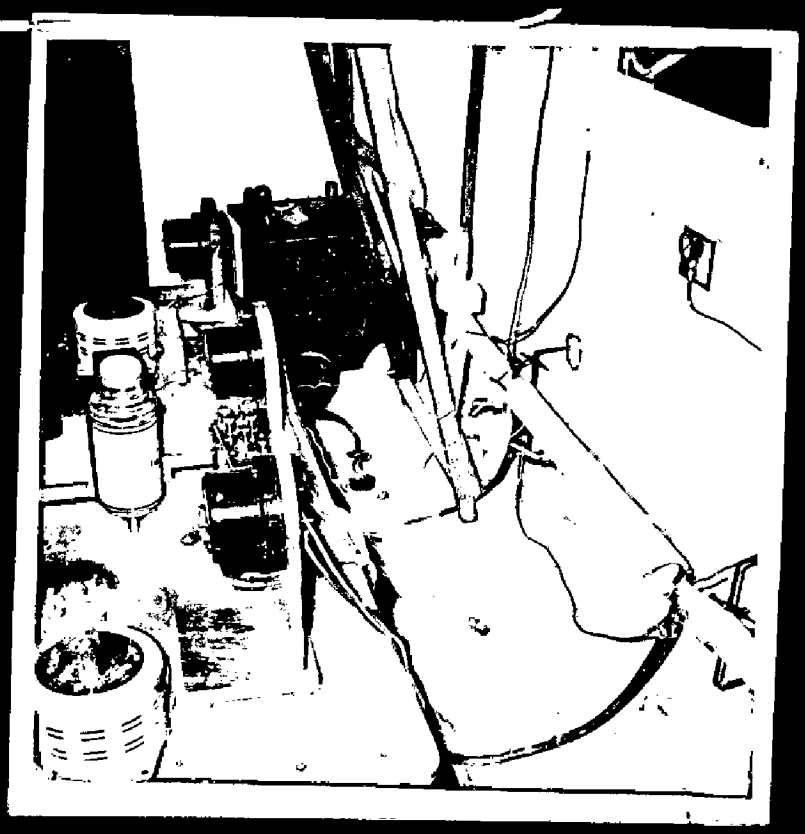

Fig. 4(ii) A view of Evaporator

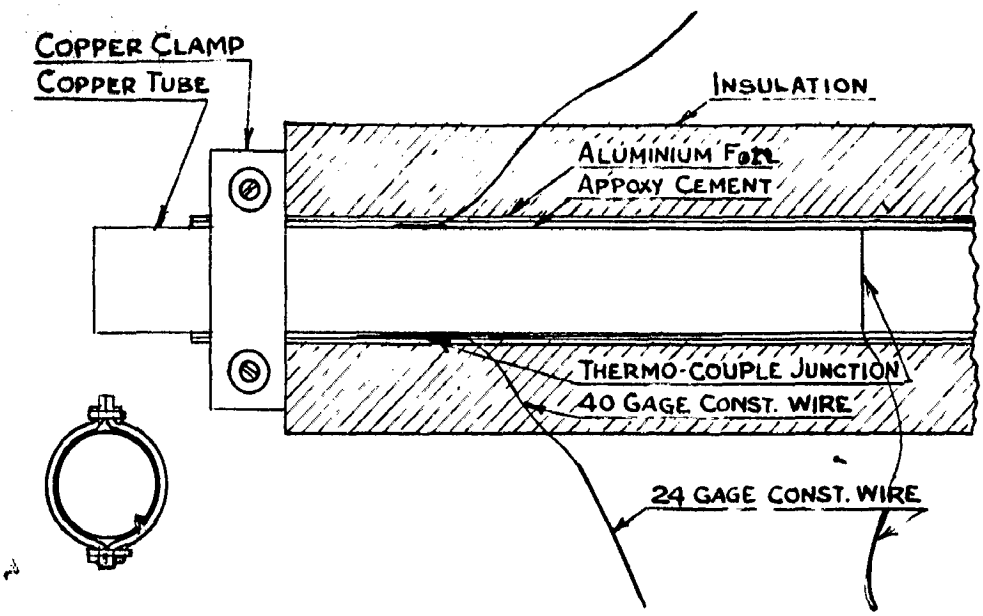

Fig 4.. TEST SECTION WITH THERMO COUPLE JUNCTIONS AND CLAMP FOR ELECT. HEATING

Liquid line and vapour line were selected as 3/8" and 7/8" O.D.Copper tubes respectively.

4.5 DESCRIPTION OF THE APPARATUS.

A schematic diagram of the apparatus is shown in Fig. 4.2 and a photographic view is given in Fig. 4.(1). The following is the key of Fig. 4.2:-

A- Ammeter	AH- After Heater.
C- Condenser	CV- Charging Valve.
CT- Current transformer	F- Flow Control Valve.
M- Manometer	P- Pressure gage.
PH- Preheter	ST- Step down transformer.
TS- Test Section.	V- Voltmeter.
VT- Variac	W- Water cooler.
WI- Water Inlet	WO- Water Outlet.

Test Section:- The evaporator test section consisted of a

hard copper tube 3/8" I.D. and 3.5 ft. long- Thermocouple junctions were made on the tube surface using constant-on thermocouple wire (40 gauge). The tube itself acted as the second metal. The soldering of fine constanton wire was not possible. To ensure the perfect electrical contact between the wire and the surface, the wire was sticked to well cleaned surface of the tube in the required position for about 1" length, by means of an adhesive tape. The leads of these fine wires were run to a short length, insulated and protected by tape. They were then connected to an ordinary 24 gauge constanton wires to the selector switch. The test length was insulated with a thin layer of insulating material and over it was wrapped an aluminium foil. The foil was wrapped in one single piece ensuring that there was no overlapping of foil and that there was no gap left between the two edges of the foil. A uniform heat flux was thus achieved.

So as to make the heat losses to a minimum the section was insulated by thermocole and then by asbestos. A part of the test section with thermocouple junctions and insulation is shown in Fig.4.3 and a photographic view in Fig. 4.(ii).

Pre-heater- To control the state of refrigerant entering the test section a preheater was made. In this case it was not necessary to have exactly uniform heat flux. Therefore, stripped nichrome wire was used as the heating

element. The pre-heater was made of a vertical copper tube 3/8" O.D. and 12" long, insulated with a thin layer of an insulating material and wound by the nichrome wire. To make heat losses to a minimum it was insulated first with asbestos paper, asbestos cloth and finally with asbestos pulp.

<u>After-Heater</u>- It was made to completely vaporise and superheat the refrigerant passing out of the test section. A copper tube 3/8" I.D. and 8" long was used for this purpose , and was prepared in the same way as pre-heater. The position of after-heater was made vertical down the test section. It enabled the liquid refrigerant from test section to collect in the after-heater and then being evaporated in it to join the vapours rising up in the vapour line.

<u>Manometer-</u> To measure the pressure drop between the two ends of test section during boiling , a manometer with mercury was used. The glass tube obviously could not be used due to possibility of breaking at the joints with copper tubing.Therefore polyethelene tubing (inert with Fr_{-12}) 3/16" I.D. was used. The joints were filled with araldite so to ensure no leakages. One limb of the manometer was made inclined to 30° to horizontal for accessibility of observations.

<u>Pressure Gauge-</u> A compound pressure gauge was employed to measure the pressure of system.

Flow Control Valve- A hand operated flow control valve was used in the liquid line to vary the mass flow of $Freon_{-12}$.

Charging Valve- It was employed to charge the system with $Freon_{-12}$.

By pass- Between the pre-heater and test section a by pass was made to join the condenser. The passage was made of polyethylene tubing. The line was provided with a shut-off valve. The purpose of by pass was to see the boiling $Freon_{-12}$.

Condenser- It was placed at a height of 10 ft. above the evaporator and consisted of a drum 2 ft. dia. and 1'-9" high in which 40 ft. length coil was placed see fig. 4.1. The cooling was achieved by chilled water from the water cooler. When working at low evaporator pressures use of ice blocks was made. As mentioned before the condensed liquid passes out of condenser easily, due to downward slope of coil. The drum was insulated at the sides and bottom to prevent heat loss from surroundings. The whole condenser was placed on a wooden plank supported by angle iron frame embedded in the wall.

The whole of the liquid line and the space between the pre-heater, test section and after-heater was well insulated to prevent any heat losses.

Variation of Tube Angle- For varying the test section angle, the two ends were held by mild steel clamps sliding

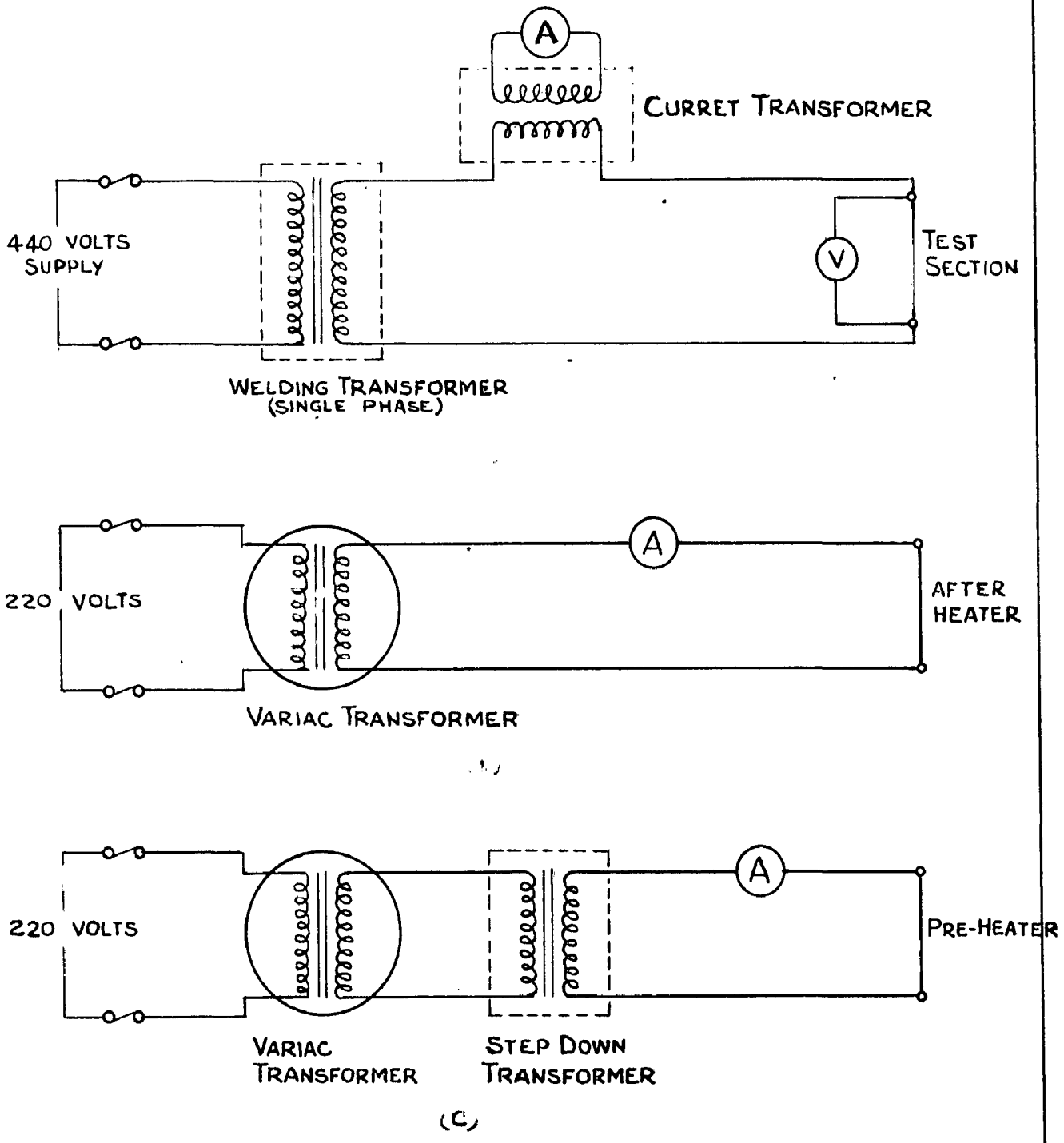

(C)

Power Supply Systems

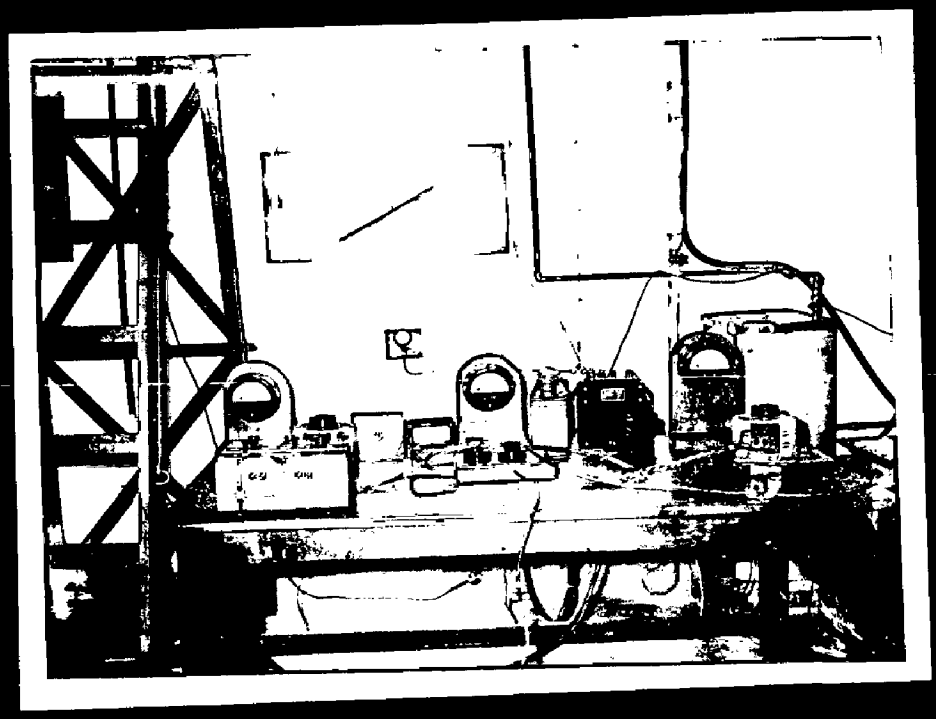

Fig.4(iii) A view of Instrumentation

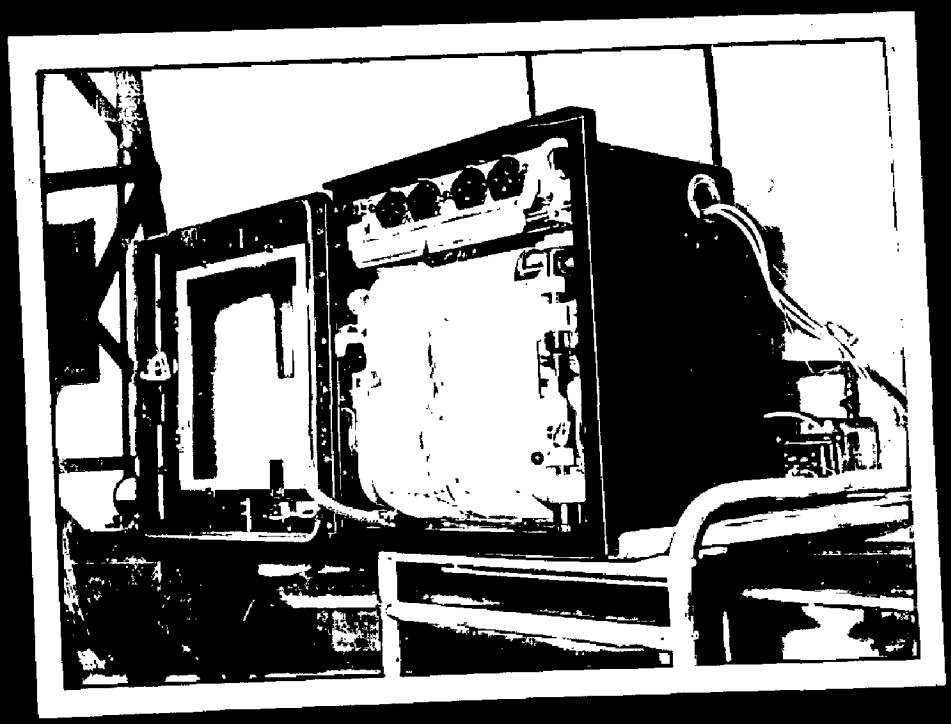

Fig. 4(iv) A view of Speedomax

up and down on two mild steel rod acting as stands, embedded in the wall. A photographic view Fig. 4(iii) shows the inclined test section with the clamps and stands at the two ends. The vertical movement of the clamps on the mild-steel rod was possible (a) due to flexibility in movement of vapour line and (b) due to coil spring of liquid line at the bottom of pre-heater.

4.6. Instrumentation.

Heat Supply System.

The test section was heated by passing electrical current through the aluminium foil. Copper conductors in the form of clamps were used as the electrical terminals at the two ends. Perfect electrical contact was achieved by keeping a thin sheet of lead between the copper clamps and aluminium foil. The electrical resistance of foil was measured as 0.0425 ohms employing double Kelvin Bridge. As the resistance was of a low order, a welding transformer was therefore used with a maximum current carrying capacity of 210 amperes., primary - 440 volts single phase. Heat fluxes to the test section were varied by varying the current output from welding transformer. Photographic view Fig. 4(iii) shows a welding transformer with other instruments. Fig. 4.4.a shows the electrical circuit diagram with the measuring instruments used.

The pre-heater was heated by passing current through copper conductors which hold the two ends of

the heating element wound over the insulated tube.

As it was not possible to give 8 amps current through auto-transformer, a step down transformer was employed to give the higher currents. Fig. 4.4 b gives the electrical circuit for preheater. The heat fluxes were varied by varying input from auto transformer.

The heat supply to after heater was made in the same way as for preheater. Fig. 4.4c gives the electrical circuit for after-heater.

The power supply to the test section, pre-heater and after heater were measured by ammeters and volt meters. It was assumed that the resistance of heaters does not vary within the temperature ranges involved. The current passing through the test section was measured by employing a current transformer and an ordinary ammeter (0-5 amps) in secondary of this transformer. The power factor for the aluminium foil was calculated as 0.95 and for each of the auxiliary heaters as 0.90.

Measurement of Mass Flow Rate.

Direct determination of mass flow rate in the absence of rotameter was not possible. It was done by reading the pressure and temperatures of $Freon_{-12}$ at points (i) before the preheater section (ii) After the preheater and before the test section. (iii) after the test section and before the after-heater- and (iv) after the after-heater. The energy balance

method was used for finding out the mass flow rate. It was assumed that there was no heat loss to the atmosphere, during the flow of $Freon_{-12}$ from preheater to the after-heater within the range of experiment.

Measurement of Temperature-

The temperatures along the test section and at other points were measured by 40 gauge constanton wire. The thermocouple wires were caliberated by Leads Northrup potentiometer. The speedomax Leads Northrup temperature recorder was used to record the temperatures directly. At A photographic view of the temperat-ure recorder with its range adjustment and zero adjustment is shown in Fig. 4(iv)

The temperature of $Freon_{-12}$ entering and leaving the test section was measured by providing thermocouples at a distance of 10" away from each end. Thus the conduction effect was reduced to a minimum. In all 12 thermocouples were used for measuring the temperatures at different points of test section.Temperatures at top and bottom of the tube were measured at four places.

The temperature of $Freon_{-12}$ at inlet to pre-heater and outlet to after-heater were achieved by insulating the thermo-couple junctions.

4.7 Test Procedure.

Before actually starting the tests the apparatus was tested for leaks by making it to withstand the pressure

of about 150 psia for 48 hours. The quantity of Freon to be charged was calculated on the basis of capacity of the system and was known at the time of charging.

[illegible]

Tests were conducted after the apparatus had been working for a sufficient period to establish equilibrium. The desired evaporator pressure was achieved by varying the cooling rate in the condenser. The liquid flow rate was charged by adjusting the flow control valve in the liquid line. The electrical input to the preheater was regulated in accordance with the quality desired at the entrance to the test evaporator. The electrical input to the after-heater was regulated so as to ensure that not only complete evaporation has taken place but a small amount of superheating is present. Energy to the test section was supplied in accordance with the change of mass flow rate and the preheater input.

After the variable (flow rate, evaporator pressure, energy input) became constant, records of temperature all along the apparatus were made, by using selector switch and the temperature recorder. The power supplied to the preheater, test section and after heater was also recorded, however on some occasions the set ones and this had to be tolerated.

Data for Horizontal Tube.

At a particular pressure, the data for horizontal tube were obtained in the following way:-

(a) Flow control valve set in a particular position.

(b) Test-section, preheater and after-heater were given an electrical input.

(c) Sufficient amount of ice was kept in the condenser so as to have the required pressure in the pressure-gage.

(d) After the pressure was constant for a considerable time, readings of thermocouple at entrance to preheater, at entrance and exit of test section after-heater and along the evaporator tube length were recorded.

(e) Pressure drop across the evaporator tube was recorded by means of mercury manometer.

(f) Mass flow rate was determined by considering energy balance at inlet to pre-heater and outlet to after-heater.

Twenty three sets of readings at various evaporator pressures were taken in the above manner to correlate the heat transfer rates and to study other factors as already mentioned previously.

Data for Inclined Tube.

The aim was not to co-relate the heat transfer data

but to study the effect of angle of tube on heat transfer rates. Therefore, tests were conducted at 0^0 5^0 and 10^0 angle of tube with horizontal, at a chosen pressure of 95 psia. Mass flow rates of 20,40, 60 and 80 lbs/hr. were selected the tests. The total number of 54 runs were made at different heat flux to the evaporator. Special care was taken to keep the evaporator pressure constant throughout all the runs. Rest of the procedure was same as for horizontal tube.

The sample calculations for the horizontal and inclined tube has been given in the appendix.

CHAPTER 5

DISCUSSION OF THE TEST RESULTS AND CONCLUSIONS

Data and test results obtained by experimentation have been discussed here. The correlation equation obtained has been compared with the data of other investigators. Pressure drop, local heat transfer coefficients, and effect of tube angle on heat transfer have been dealt with separately. In the end several conclusions have been drawn on the basis of discussion and the need for further investigation has been emphasised wherever necessary.

The results of the experiment and their discussion will be presented in the following paragraphs. The results have been tabulated in Appendix A.

The results could be best interpreted by studying the following curves drawn from the test results:-

1) A plot between $\frac{C_l \Delta T_x}{h_{fg} (N_{Pr})^{1.7}}$ vs $\frac{q/A}{h_{fg} \mu_l} \sqrt{\frac{g_o \sigma}{g(\rho_l - \rho_v)}}$

for horizontal tube for the entire range of experiment to give a correlation equation.

2) A plot between log q/A and ΔT_x for horizontal tube to show the effect of ΔT_x on heat transfer rates.

3) Plots of tube surface temperature and local heat transfer coefficient against the distance from evaporator inlet for horizontal and inclined tube to show the variation along tube length.

4) A plot of h_{avg} and ΔT_x for some two particular evaporator pressure to show the effect of evaporator pressure on heat transfer rates.

5) A plot of N_{Nu} Vs $\frac{P}{(L/D)}$ for the entire range of the horizontal tube to show the relationship of pressure drop during boiling with the heat transfer rates.

6) A plot of mass flow rates and P for the entire range of horizontal tube to show the effect of mass flow rate on pressure drop.

65 - 77 PSIA ⊙
80 - 85 PSIA X
88 - 97 PSIA ⊠
93 - 103 PSIA △
105 - 120 PSIA ⊡

EVAPORATOR TUBE 3/8" I.D. 3·5 FEET LONG
TUBE – HORIZONTAL

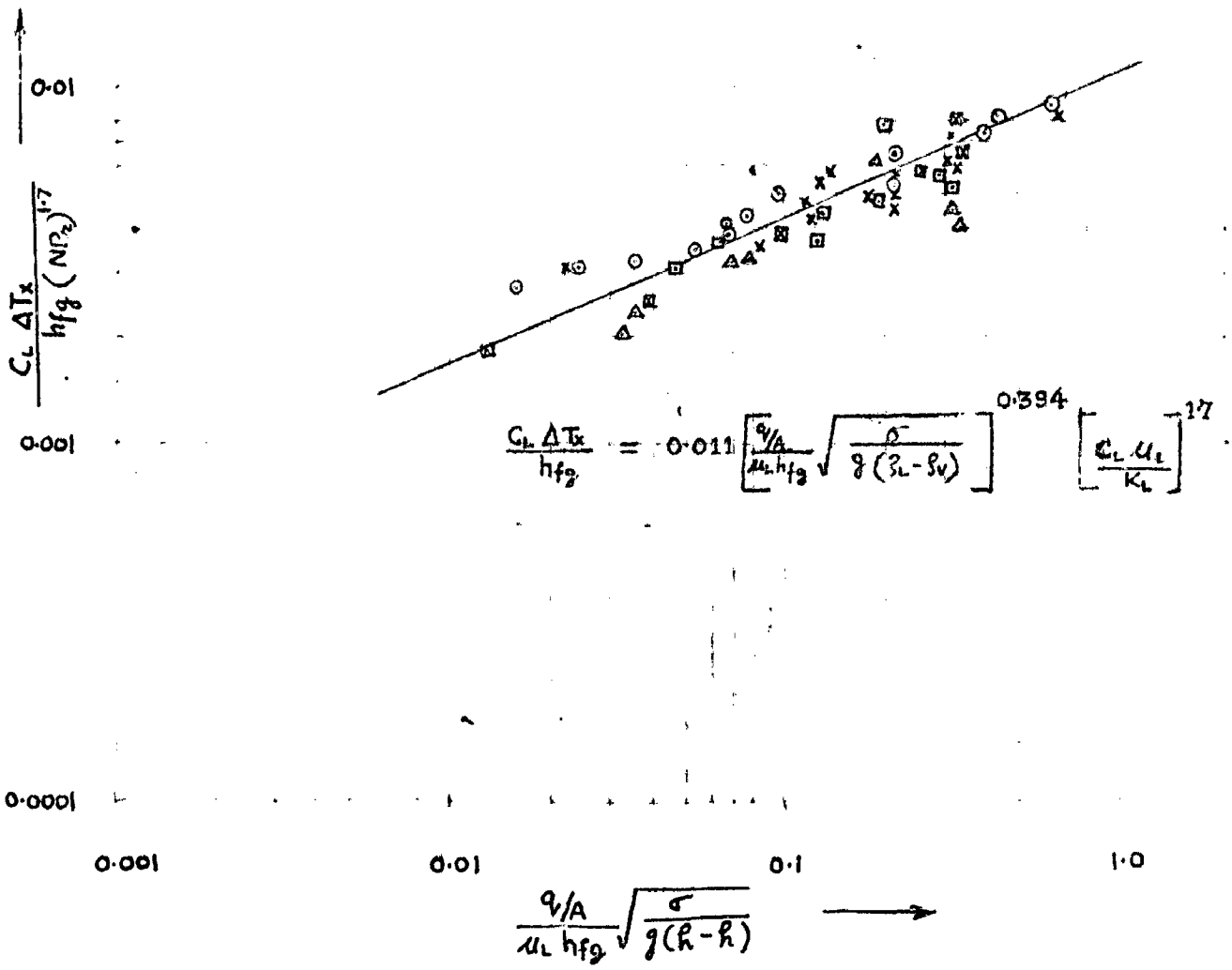

$$\frac{C_L \Delta T_x}{h_{fg}} = 0.011 \left[\frac{q/A}{\mu_L h_{fg}} \sqrt{\frac{\sigma}{g(\rho_L - \rho_v)}}\right]^{0.394} \left[\frac{C_L \mu_L}{K_L}\right]^{1.7}$$

7) A plot of h_a and tube angle with horizontal to show variation of heat transfer with tube angle.

8) Plots of ha Vs q/A for different tube angles and different mass flow rates to show variation of heat transfer coefficient with heat flux.

Correlation Equation-

To obtain the correlation of the form,

$$\frac{C_l \Delta T_x}{h_{fg}} = C_{sf}\left[\frac{q/A}{h_{fg}\mu_L}\sqrt{\frac{g_o\sigma}{g(\rho_L-\rho_v)}}\right]^n\left[\frac{C_l\mu_L}{K_L}\right]^s$$

the convention is to plot $\frac{C_l \Delta T_x}{h_{fg}(N_{Pr})^{1.7}}$ against $\frac{q/A}{\mu_L h_{fg}}\sqrt{\frac{g_o\sigma}{g(\rho_L-\rho_v)}}$

As a result of the experiments conducted by Addoms for pool boiling, the value of $s = 1.7$ was determined by a cross plot of $\frac{C_l \Delta T_x}{h_{fg}}$ versus N_{pr} for constant values of bubble Reynolds Number. Hence, value of s was taken to be 1.7 . Fig. 5.1 reveals the method of correlation in the form mentioned above is reasonably successful.

The following correlation equation has been obtained for temperature differentials less than $12^{0}F$ and mass flow rate: less than 120 lbs/hr.

... 5.1

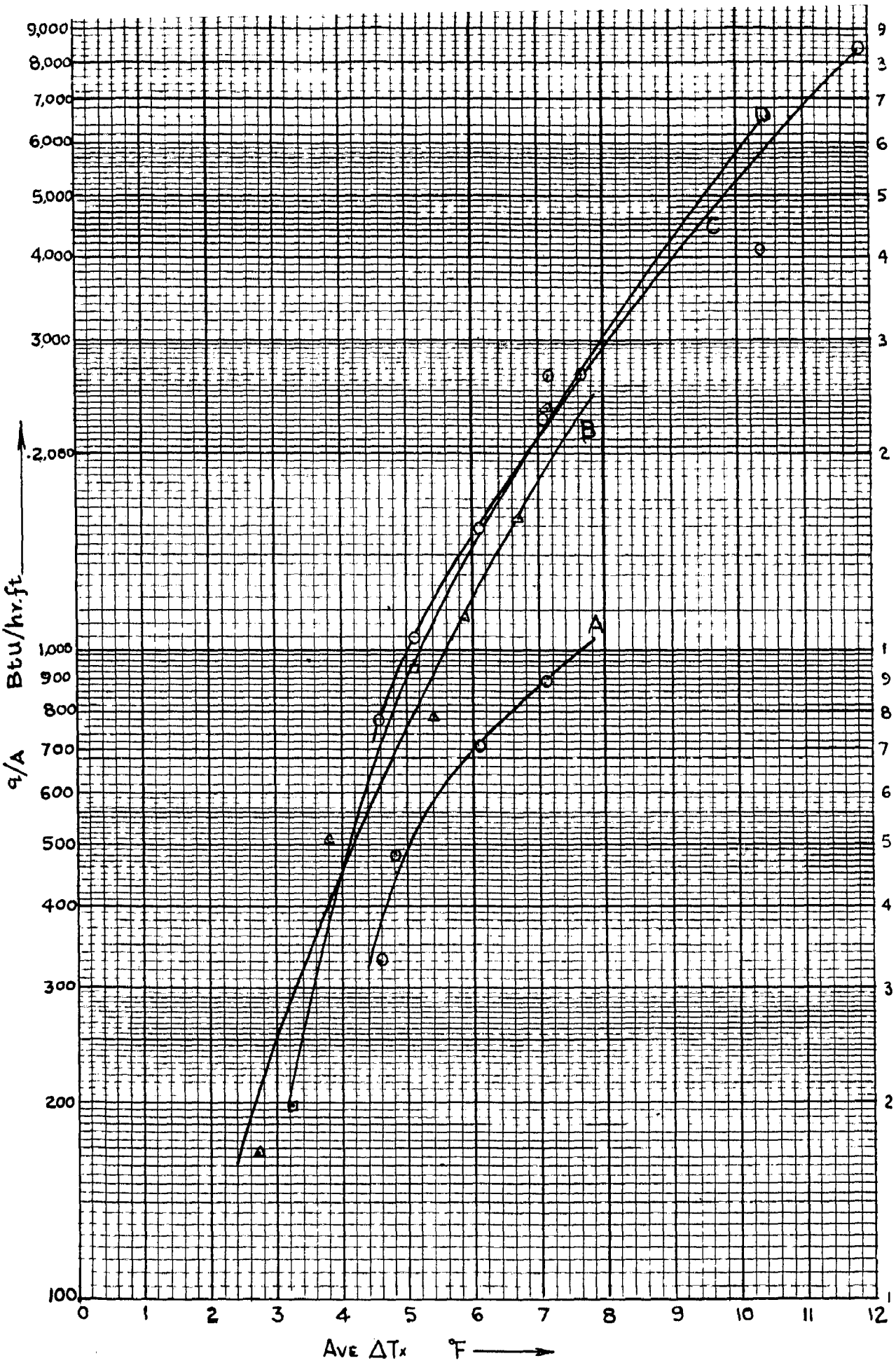

FIG. 5.2 EFFECT OF ΔTx ON HEAT TRANSFER RATES

CURVE A - 62°F SAT. TEMP.
CURVE B - 77.5°F " "
CURVE C - 70°F " "

Baker, Foulkins and Hawkins[26] in their experimental investigation of boiling Pr_{-12} in horizontal evaporator tube, correlated the data and determined the value of C_{sf} and r as 0.0125 and 0.333 respectively. Probably the most significant cause of difference in the value of C_{sf} of the author and above investigators is due to the fact that C_{sf} is a function of β which is determined by the character of and kind of heating surface and by the properties of the fluid. Additional information regarding the value of β is , therefore, necessary for reaching an agreement. The difference in the value of exponent r is probably in determining the accurate value of ΔT_x. As will be seen latter, that q/A rises rapidly with small changes in ΔT_x. The value of ΔT_x is obtained by subtracting the saturation temperature from the determined heating surface temperature. A small error in reading the evaporator pressure and consequently the saturation temperature will change the value of ΔT_x and would thus affect the term $\frac{C_{pf}\,\Delta T_x}{h_{fg}}$. However, the difference in the two values does not seem to be discouraging.

Temperature Differentials.

Fig. 5.3 shows a plot of $\log q/A$ versus ΔT_x for the four different evaporator pressures. It is observed that q/A rises rapidly with small changes in ΔT_x.

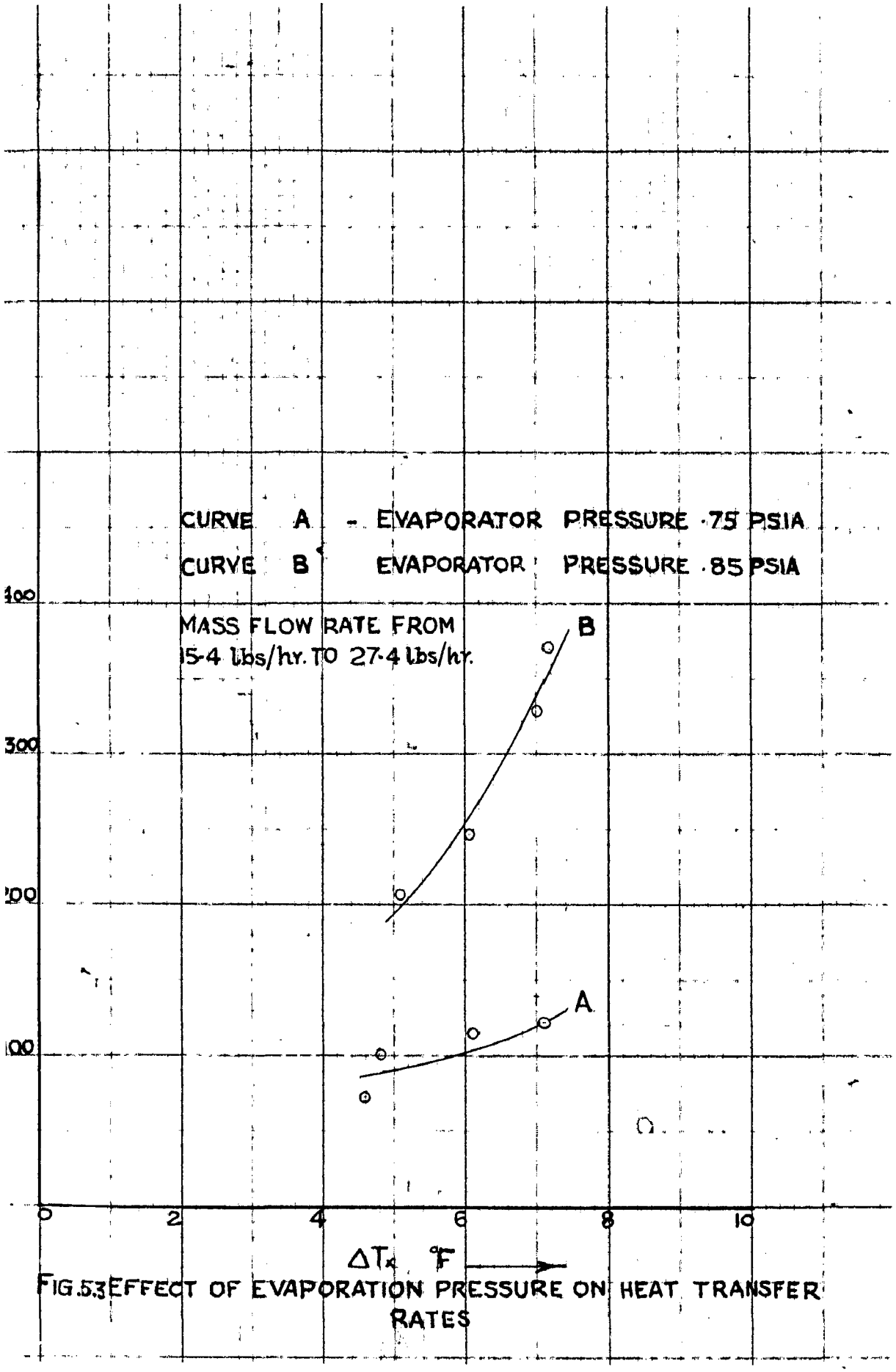

FIG.5.3 EFFECT OF EVAPORATION PRESSURE ON HEAT TRANSFER RATES

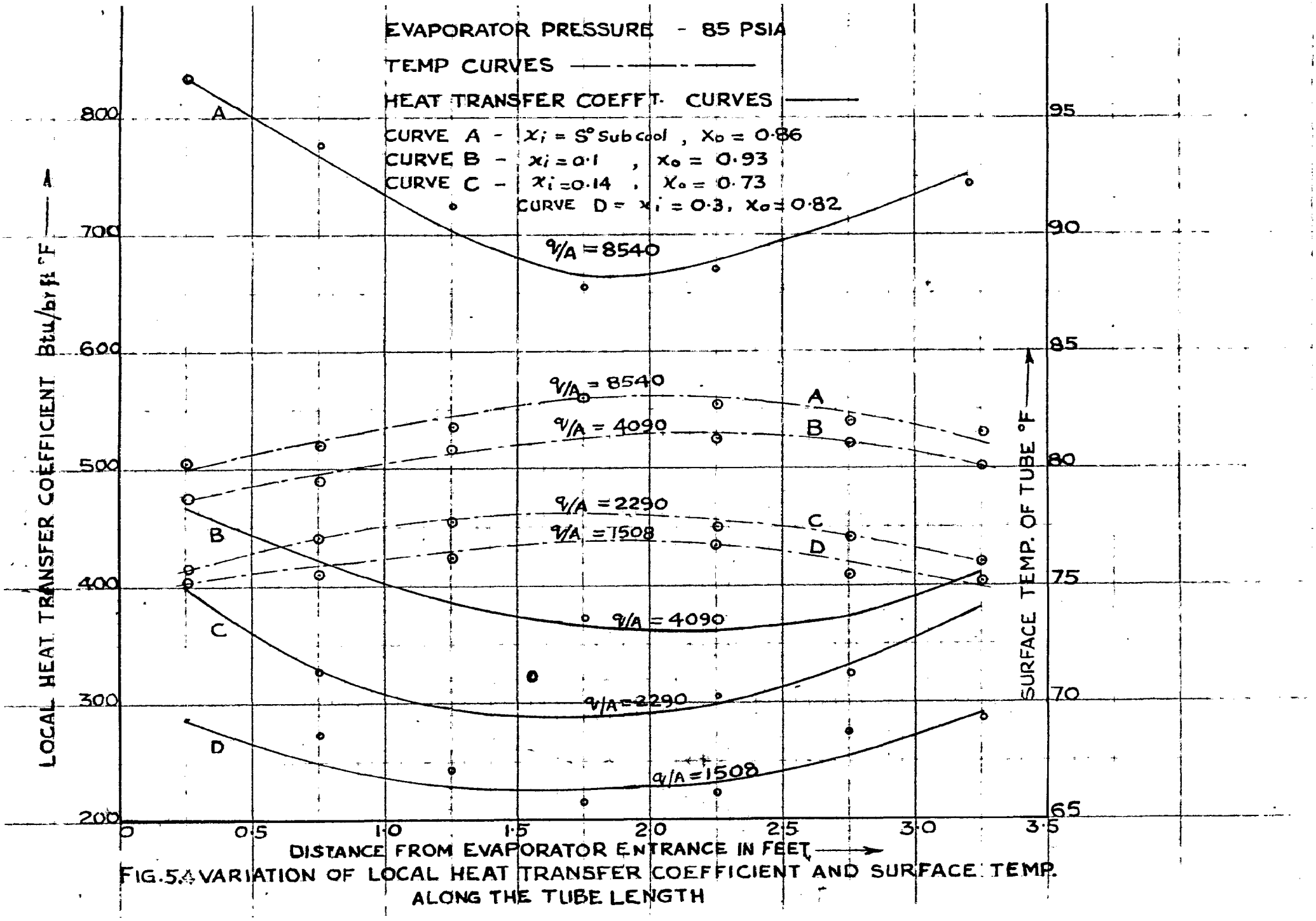

FIG. 5.4 VARIATION OF LOCAL HEAT TRANSFER COEFFICIENT AND SURFACE TEMP. ALONG THE TUBE LENGTH

It may be said that ΔT_x is the driving force for the heat transfer. The curves are in agreement with the region of nucleate boiling.[16]

Evaporator Pressure.

Study of Fig. 6.3 which is a plot of h_o vs ΔT_x for two different evaporator pressure indicates that for a given temperature difference and mass flow rate, the heat transfer increases as the evaporator pressure is increased. It is in agreement with the work of other investigators discussed in Chapter 1.

Local Heat Transfer Coefficients.

It is of interest to study the distribution of the local coefficient of heat transfer along the length of test section. Fig.6.4 shows the distribution of local coefficient and the surface temperature of evaporator, when the tube was horizontal. The curves indicate that heat transfer at first decreases and then increases towards the end. This may be attributed to the fact that as the refrigerant enters the tube, boiling starts with the vapour phase in laminar flow. As the boiling proceeds along the length of the tube, more and more amount of vapour is thus reducing the wetted area and consequently reducing the heat transfer rate. It may be predicted that a stage is reached when the turbulence starts and again the heat

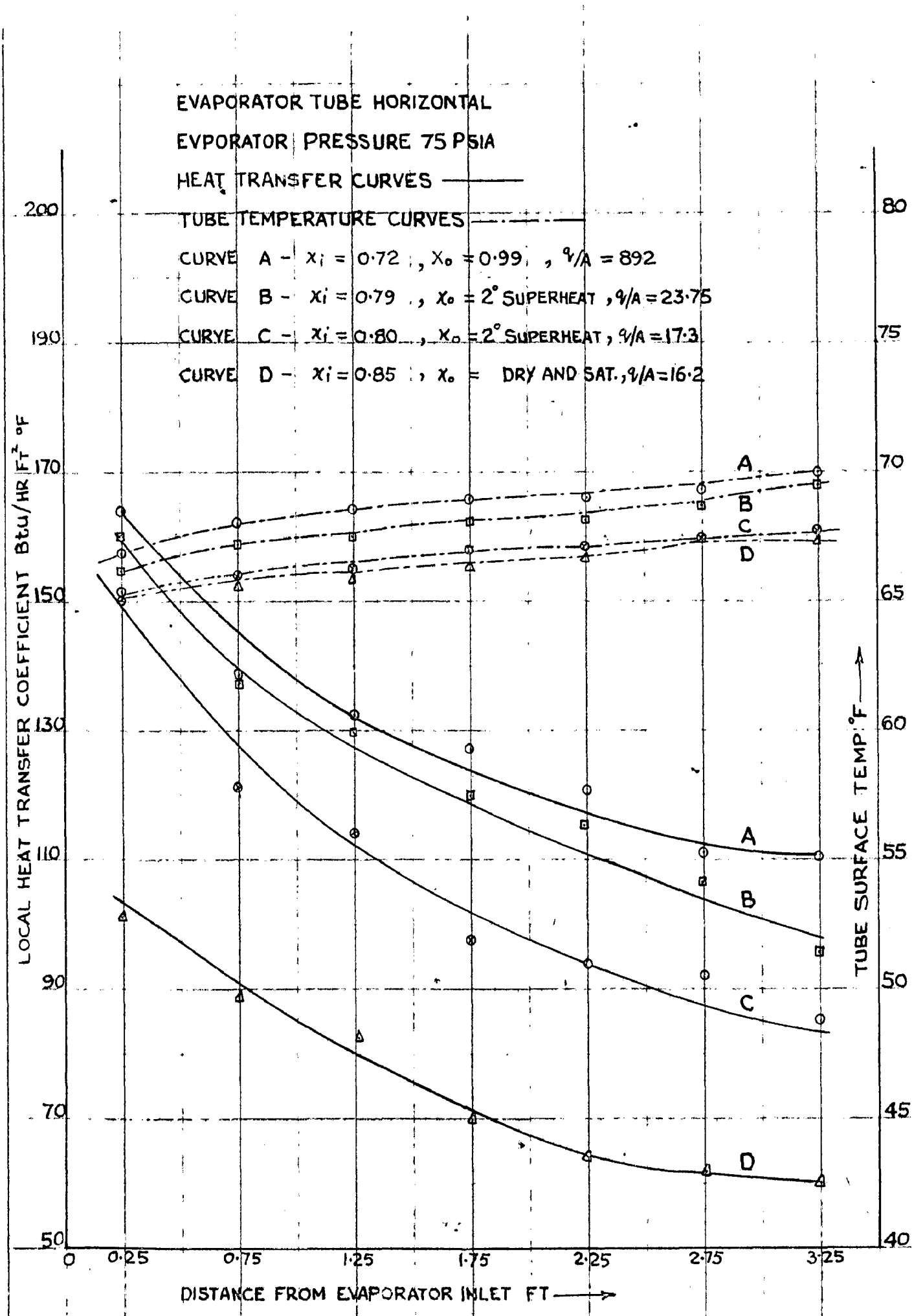

FIG.5.5 VARIATION OF LOCAL HEAT TRANSFER COEFFICIENT AND SURFACE TEMPERATURE ALONG TUBE LENGTH.

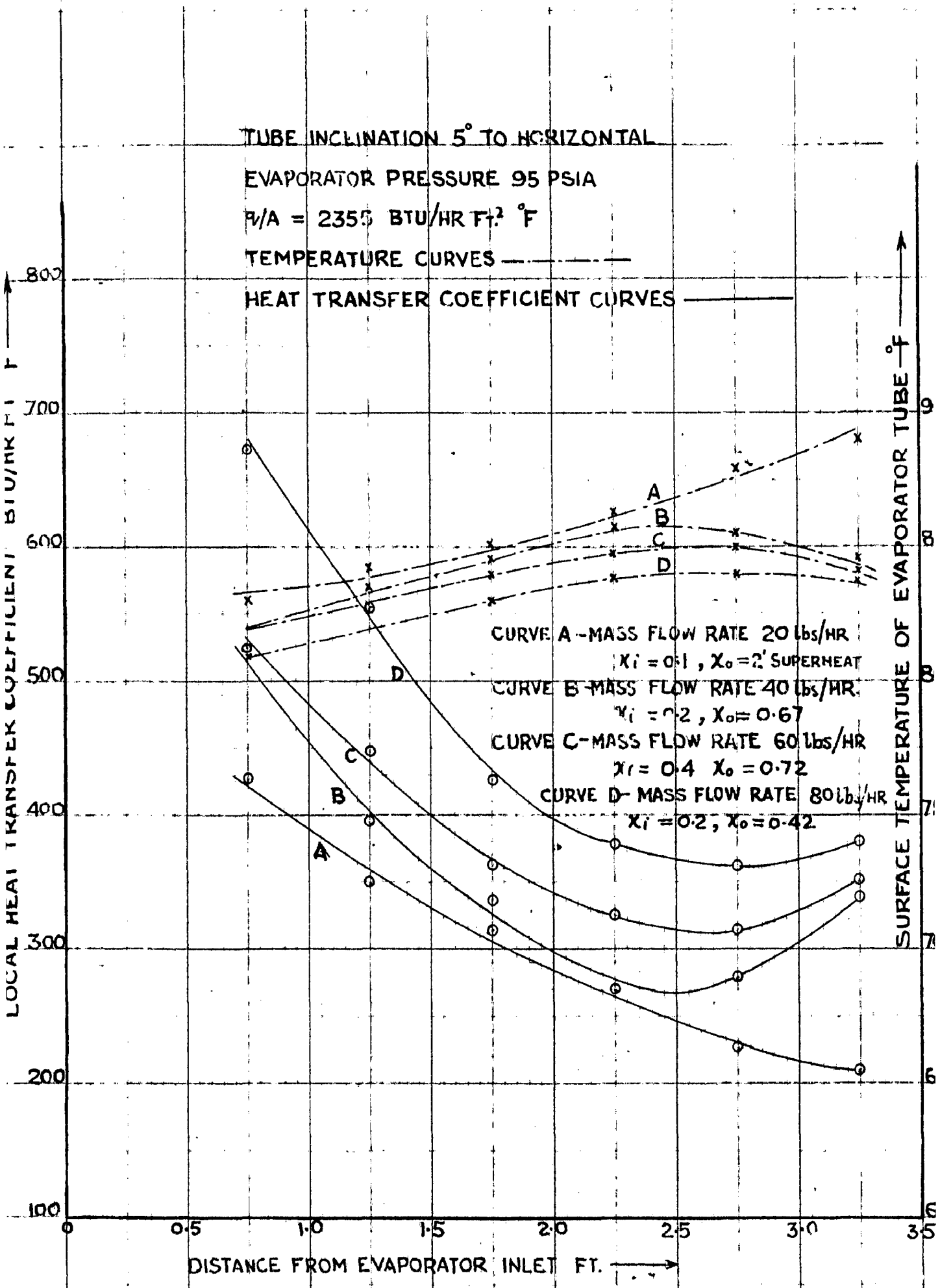

FIG. 5.6 VARIATION OF LOCAL HEAT TRANSFER COEFFICIENT AND SURFACE TEMPERATURE ALONG TUBE LENGTH

TUBE INCLINATION 10° TO HORIZONTAL

EVAPORATOR PRESSURE - 95 PSIA

MASS FLOW RATE : 40 lbs/hr

TEMPERATURE CURVES ——·——·——

HEAT TRANSFER CURVES ————

CURVE A - $q/A = 4220$ BTU/HR FT^2, $x_i = 0.14$, $x_o = 2°$ SUPER HEAT

CURVE B - $q/A = 3170$ BTU/HR FT^2, $x_i = 0.15$, $x_o = 0.77$

CURVE C - $q/A = 2355$ BTU/HR FT^2 $x_i = 0.2$, $x_o = 0.67$

CURVE D - $q/A = 1182$ BTU/HR FT^2 $x_i = 0.4$, $x_o = 0.64$

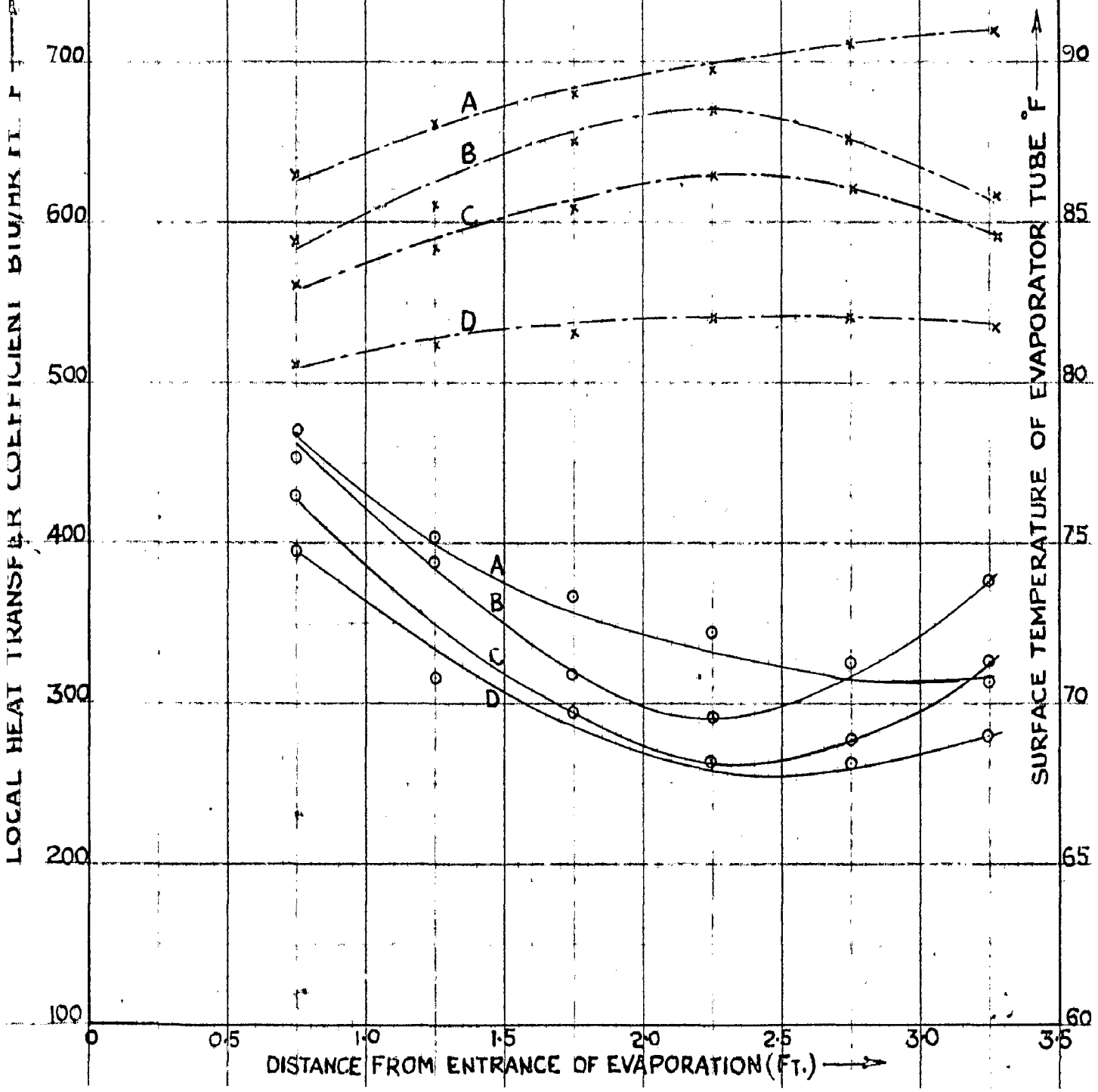

transfer is increased. Therefore, it appears that much will depend upon the condition of refrigerant entering and leaving the evaporator tube. The four curves in Fig.5.4 represent the different entering and leaving conditions with the corresponding heat flux. It is further to be noted that due to increased amount of vapour portion at the outlet of evaporator, the heat transfer coefficient is less than that at the inlet. The exception is curve D which represents about same value of heat transfer coefficient at both ends. Fig. 5.5 represents the heat transfer and tube temperature curves when more than 70% of the refrigerant is in the form of vapour at the time of entering the evaporator tube. Curves B and C represent the superheating in the part of the evaporator. The heat transfer has continuously decreased from one end to other end. Curves A and D represen saturated condition at exit end. In each case the heat transfer has decreased. The effect of turbulence seems to be non-prevalent in comparison with the decrease of wetted area.

Fig. 5.6 and 5.7 represent the distribution of local coefficients in inclined tube. The curves of Fig.5.6 have been drawn at a particular heat flux and for varying mass flow rate. It is to be noted that with increasing mass flow rates, the heat transfer coefficient increases. Curve A superheating in the part of evaporator. The curves of Fig.5.7 have been drawn at a particular mass flow rates and for varying heat fluxes. Heat transfer coefficient first decreases and then increases

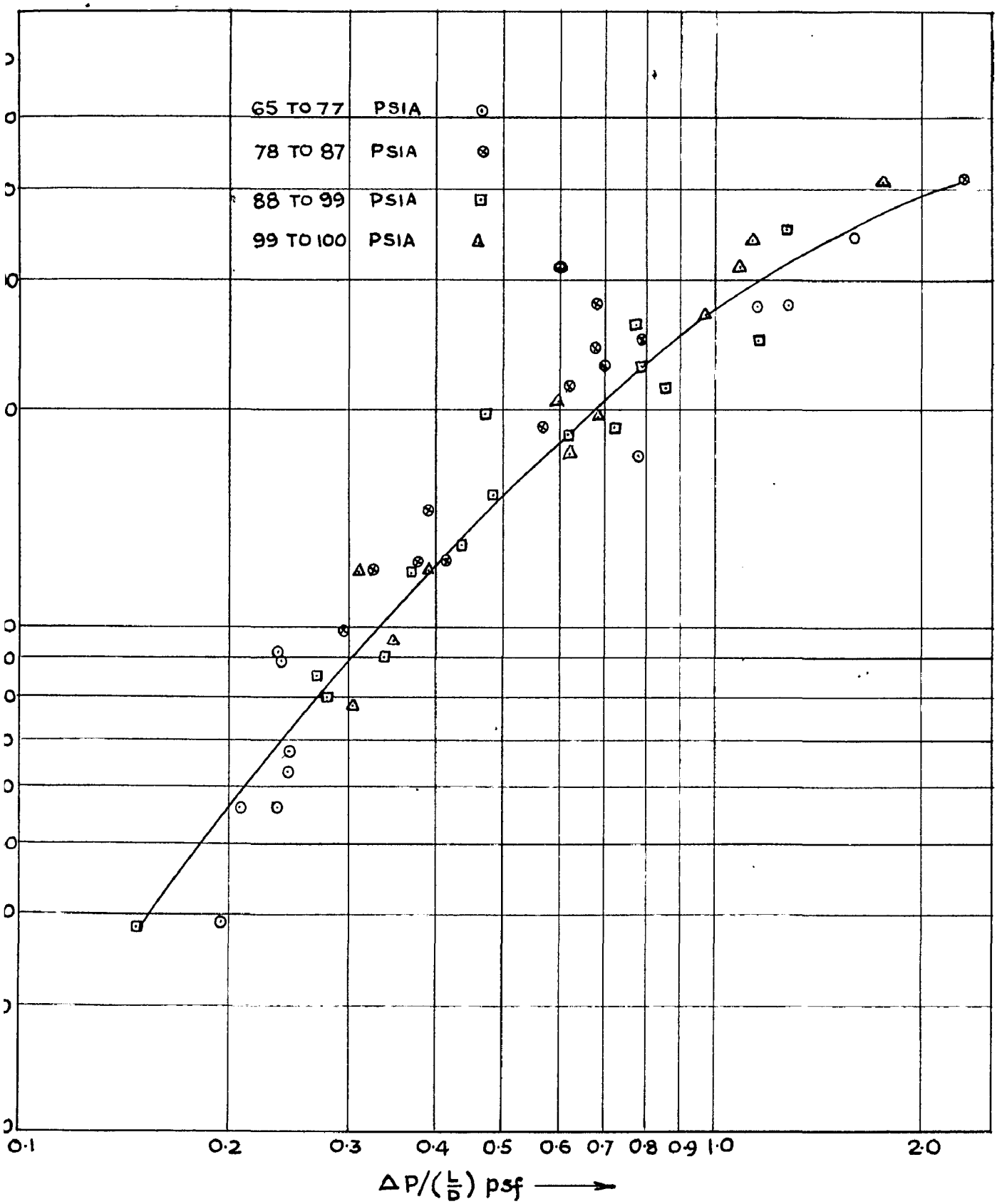

FIG. 5.8 HEAT TRANSFER AS RELATED TO PRESSURE DROP

as seen in previous cases, except for the Curve A.

The place of minimum heat transfer appears to be different in horizontal and inclined tube. The average position of minimum heat transfer in case of horizontal tube appears to be 3 ft. from inlet whereas it appears to be 2.5 ft. in case of inclined tube. Additional data is necessary before this could be generalised. However, one thing is common for both that the curves become more flat as the dryness fraction at entrance of evaporator increases.

Heat Transfer and Pressure Drop.

It was not possible to correlate the data to give a generalisation of results. However N_{Nu} and pressure gradient have been plotted in Fig. 5.8 for the entire range of experiment. The correlation on this basis is in the form of the curve the gradient of which decreases as pressure gradient increases. Bryan and Quaint[25] correlated the heat transfer and pressure drop data for Freon$_{-11}$ by plotting $\frac{h}{k}$ Vs $P/(\frac{L}{D})$. A similar type of curve was observed. The slope of best straight line drawn through the data of Bryan and Quaint was 0.73. Ashley data similarly plotted gave the slope as 0.7. The author has found a slope of 0.8 for the best straight line drawn through the data plotted in Fig.5.8.

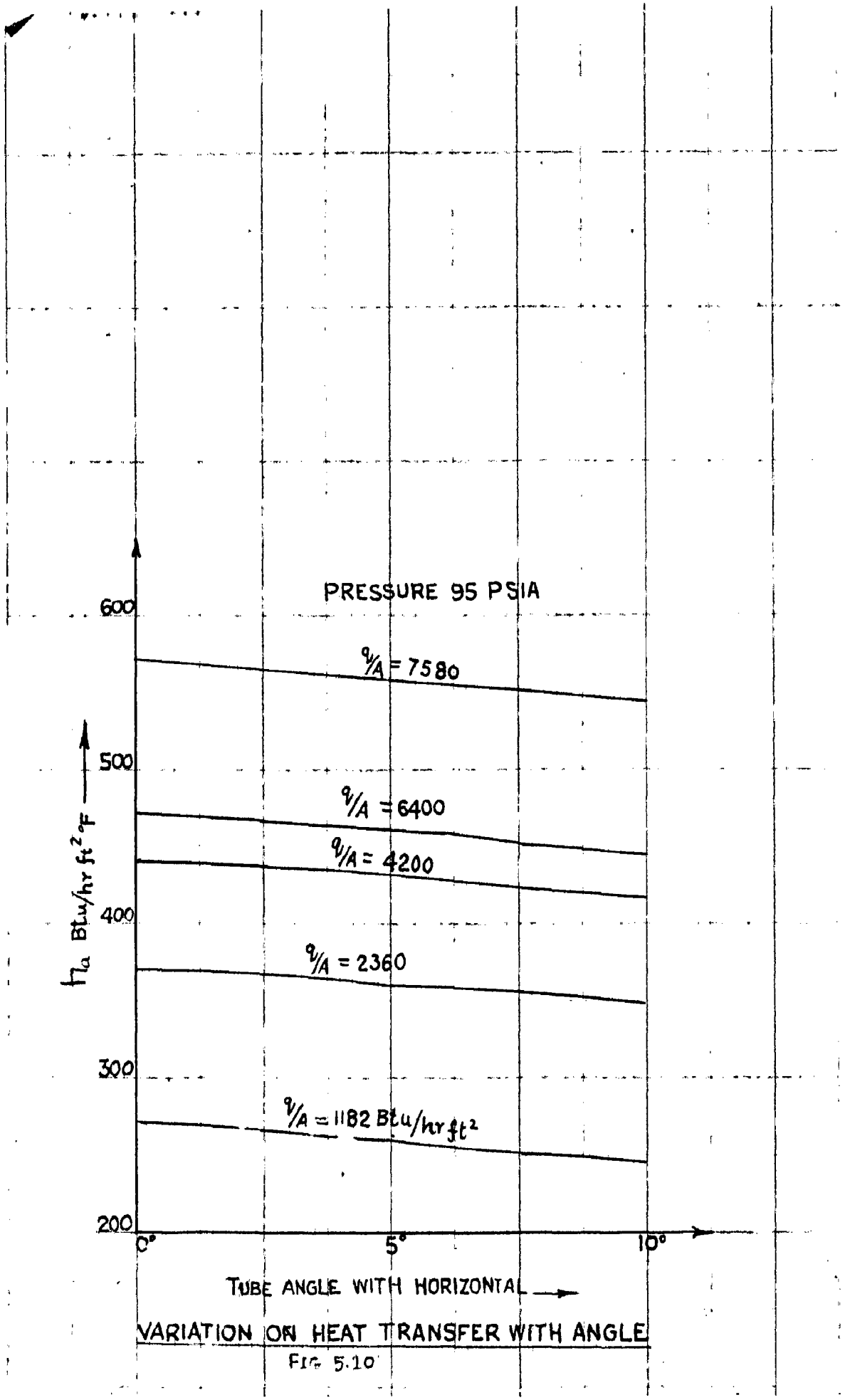

VARIATION ON HEAT TRANSFER WITH ANGLE

FIG 5.10

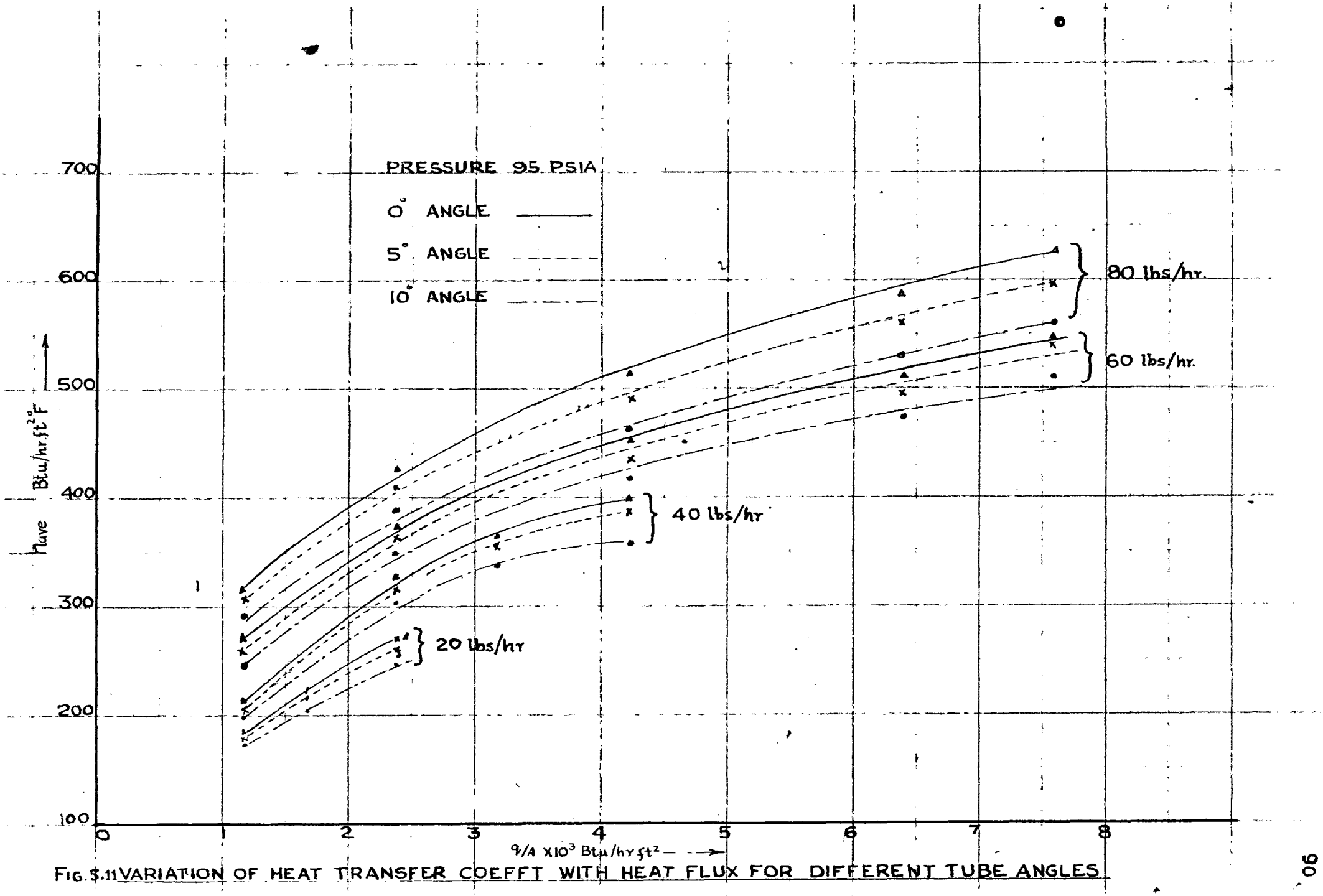

FIG. 5.11 VARIATION OF HEAT TRANSFER COEFFT WITH HEAT FLUX FOR DIFFERENT TUBE ANGLES

Mass Flow Rate and Pressure Drop:-

Fig. 5.9 represents the mass flow rate plotted against pressure drop. The scattering of points at low mass flow rate indicates that a correlation is not possible for this range. At mass flow rates greater than 30 lbs/hr a correlation has been obtained. The slope of the straight line drawn through the data plotted is 0.84. The author has not been able to find out the data of other investigators for this plot. It may be noted that at any increase of mass flow rate in the region of lower mass flow rate is not followed by the increase in pressure drop.

Heat Transfer rates and Tube Angle:

As pointed out in the beginning the author has been interested to study the effect of variation of tube angle on the heat transfer. It has not been possible to go for angle more than 10^{0} due to the limitation of the apparatus.

Fig. 5.10 represents the plot of h_{ave} versus tube angle for different heat fluxes. The heat transfer coefficient decreases as the tube angle increases. The plot is not very much satisfactory as the data could be taken only at three angles 0^{0}, 5^{0} and 10^{0}.

Fig. 5.11 represents the data for inclined tube in a more informative way. Average heat transfer coefficients have been plotted against heat flux for the different mass flow rates and different tube angles. The following points

[illegible]be observed from the figure-

1) For the same heat flux h_{ave} increases as the mass flow rate increases.

2) For the same mass flow rate h_{ave} decreases as the tube angle increases.

3) The decrease of h_{ave} between 5^0 and 10^0 is more than the decrease between 0^0 and 5^0.

All the curves show the above points consistently. The decrease of heat transfer with increase of tube angle may be due to the reason that for same mass flow rate, the velocity of vapour phase will decrease with the small increase of angle with horizontal. How far it may be true with greater angles can not be said. The decrease of heat transfer more predominant between 5^0 and 10^0 may be due to above mentioned point.

Before a generalised statement may be made additional data is necessary to elaborate this point further.

CONCLUSIONS.

On the basis of experimental data and the discussion of its results following conclusions may be drawn-

1) The boiling of Fr_{-12} in horizontal tube may be represented by the equation 5.1 for mass flow rates less than 120 lbs/hr. and temperature differentials less than 18^0F, which includes

the entrance of sub-cooled liquid and liquid with a dryness fraction also.

2) The temperature differential between the heating surface and boiling liquid is important from the point of view of heat transfer.

3) Heat transfer coefficient increases with the increase of evaporator pressure.

4) Heat transfer coefficient increases with the mass flow rate and q/A, the both increasing simultaneously.

5) Local heat transfer coefficient first decreases and then slightly increases along the length of evaporator tube for incomplete evaporation, but continuously decreases when complete evaporation and superheating takes place. The variation of local heat transfer coefficient becomes less predominant when the dryness fraction of liquid entering the evaporator increases. The place of minimum heat transfer shifts towards the end as the tube is made inclined to horizontal. However, additional experimentation is needed to study it.

6) Heat transfer rate increases with the pressure drop in evaporator. At higher pressure drops the increase is not proportional.

7) At lower mass flow rates pressure drop does does not increase much. At mass flow rates greater than 30 lbs/hr, the pressure drop is proportional to the mass flow rates.

8) Heat transfer decreases with the increase of tube angle. It is difficult to generalise this statement with the information available here. Additional experimentation is needed to study it.

The above conclusions does not make the study of this subject complete, but however, give us an insight into it. Further work is needed to obtain consistent data with respect to progressive vaporization . The inclination of evaporator tube angle still poses the problem which may be seen by additional experimentation.

APPENDIX A

TABLE A - 1

RESULTS FOR THE HORIZONTAL TUBE

Run No	Evaporator Pressure psi (Sat Temp ^{o}F)	Heat Flux q/A Btu/hr ft^2	Mass Flow Rate lbs/hr	Average Temp Diff Bet Tube Wall & Point Tx ^{o}F	$\frac{C_L \Delta T_x}{h_{fg}}$	$\frac{q/A}{h_{fg}\mu_L}\sqrt{\frac{g}{g(\rho_L-\rho_v)}}$	$\frac{C_L \mu_L}{K_L} = N_{pr}$	$\frac{C_L \Delta T_x}{h_{fg}(NP_r)^{1.7}}$
2	3	4	5	6	7	8	9	10
1	65	5440	94.8	9.7	0.0349	0.43	2.33	0.00825
2	(53)	2660	47.5	7.6	0.0275	0.211	2.33	0.0065
3		952	20.0	5.1	0.0185	0.075	2.33	0.00438
4		196	5.16	3.2	0.0116	0.015	2.33	0.00237
1	70	7580	119	11.3	0.0419	0.622	2.46	0.00869
2	(58)	4610	83.5	9.3	0.0341	0.395	2.46	0.00735
3		1152	21.5	6.3	0.0228	0.095	2.46	0.00493
1	75	892	24.6	7.2	0.0229	0.065	2.73	0.00415
2	(62)	712	23.7	6.1	0.019	0.052	2.73	0.00345
3		483	17.3	4.8	0.0178	0.035	2.73	0.00324
4		328	16.2	4.6	0.0171	0.024	2.73	0.00311
1	77 (64)	845	18.2	5.2	0.0194	0.066	2.56	0.00386
1	60	4130	38.3	8.1	0.0306	0.325	2.62	0.00506
2	(66)	2700	33.5	6.2	0.0233	0.212	2.62	0.00454
3		1605	30.19	7.4	0.0279	0.126	2.62	0.00543
1	81 (67)	1432	22.2	6.6	0.0249	0.112	2.65	0.00475

2	3	4	5	6	7	8	9	10
1	83	4150	44	9.8	0.0372	0.212	2.81	0.00554
2	(68)	1960	28.2	8.2	0.0311	0.133	2.81	0.00587
1	85	8540	72.6	11.8	0.0452	0.666	2.71	0.0083
2	(70)	4090	37.8	10.3	0.0395	0.319	2.71	0.00725
3		2660	27.4	7.2	0.0274	0.208	2.71	0.00504
4		2290	29.6	7.0	0.0263	0.179	2.71	0.00492
5		1508	18.8	6.1	0.0233	0.118	2.71	0.00428
6		1056	15.4	5.1	0.0195	0.082	2.71	0.00359
7		778	13.4	4.6	0.0175	0.022	2.71	0.00315
1	88 (72.5)	2465	54.3	11.4	0.0439	0.103	2.74	0.00785
1	89	4260	39.5	9.6	0.0372	0.333	2.74	0.00369
2	(73)	4125	61.5	11.5	0.0445	0.323	2.74	0.0080
1	90	4090	44.7	10.8	0.0417	0.319	2.75	0.00659
2	(74)	2290	17.3	7.0	0.0271	0.181	2.75	0.00486
1	93	2450	28.25	8.2	0.0321	0.212	2.81	0.00554
	(76)	1492	30.9	6.5	0.0254	0.125	2.81	0.0044
1	95	2315	37.0	7.4	0.0291	0.181	2.83	0.00495
2	(77.5)	1004	20.1	6.6	0.0261	0.125	2.83	0.00445
3		1130	16.4	5.8	0.0228	0.096	2.83	0.00388
4		800	13.92	5.4	0.0212	0.062	2.83	0.00301
5		498	9.02	3.8	0.0145	0.039	2.83	0.00247
6		160	6.52	2.7	0.0106	0.012	2.83	0.00181

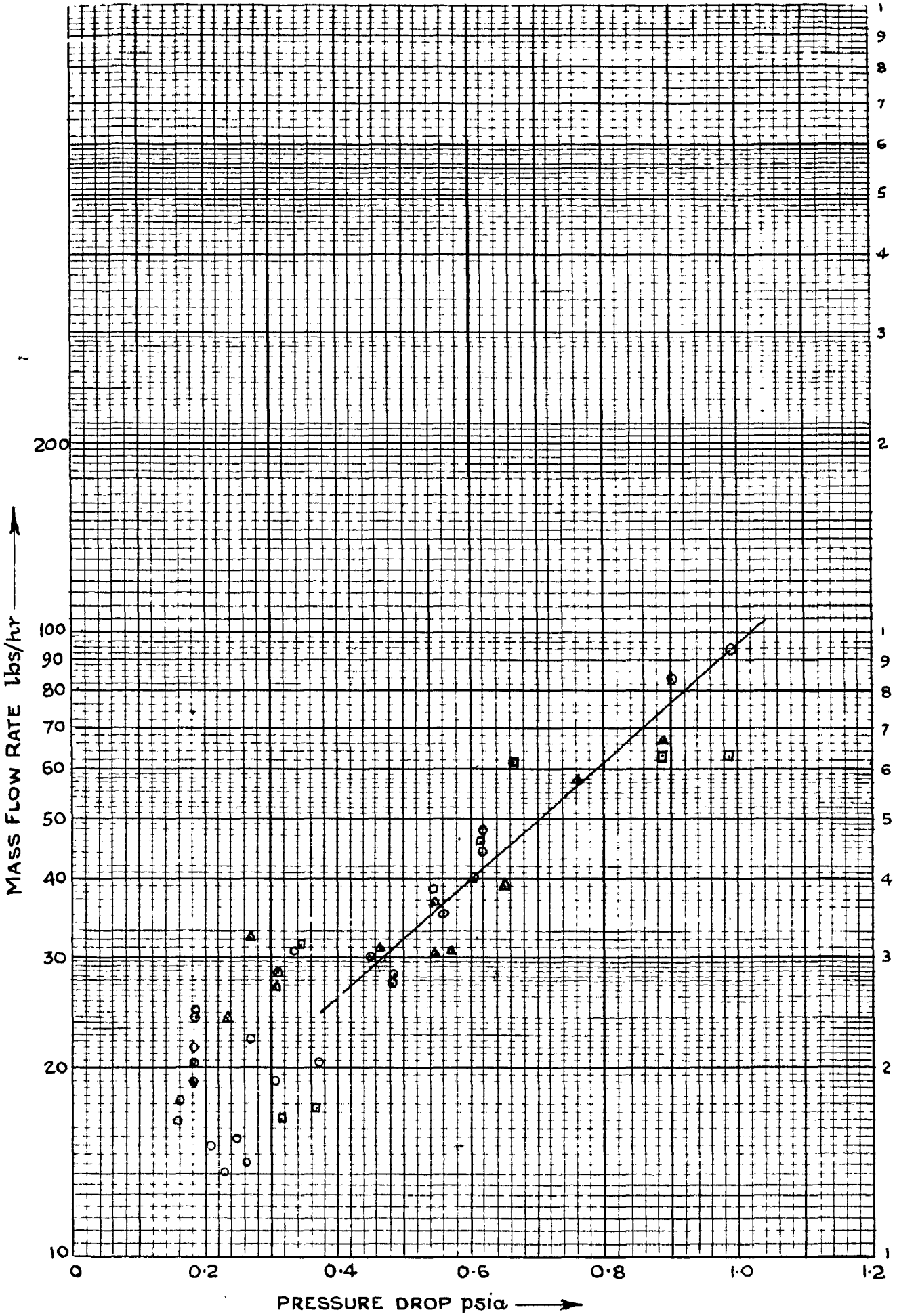

FIG. 5.9 EFFECT OF MASS FLOW RATE ON PRESSURE DROP

PRESSURE 65 TO 80 PSIA
84 TO 87 PSIA

2	3	4	5	6	7	8	9	10
1	97 (79)	3170	62.5	7.9	0.0311	0.250	2.83	0.0053
1	98 (79.5)	4000	60.7	7.0	0.0275	0.311	2.87	0.00458
2		419	14.85	3.0	0.0121	0.033	2.87	0.00201
1	100 (81)	4090	30.7	6.1	0.0245	0.333	2.88	0.00406
2		850	9.3	5.0	0.0199	0.077	2.88	0.0033
3		436	23.8	3.8	0.0143	0.035	2.88	0.00237
1	102 (82)	895	27.1	4.8	0.0192	0.038	2.80	0.0032
1	103 (83)	2455	34.8	8.9	0.0357	0.189	2.88	0.006
2		2360	31.9	7.3	0.0293	0.161	2.88	0.0049
1	105 (84)	4000	58.4	9.4	0.0378	0.306	2.82	0.0061
1	109 (86.5)	615	32.3	4.1	0.0167	0.047	2.93	0.00308
1	110 (87)	4130	39.5	8.5	0.0347	0.294	2.93	0.00568
1	116 (91)	1075	30.2	5.6	0.0232	0.126	2.95	0.0037
1	120 (93)	4130	66.2	8.0	0.0336	0.31	2.97	0.00525

TABLE A-1 (Contd)

Data and Results for Horizontal Tube.

Run No.	Pressure psia. (Satn. Temp $^{\circ}F$)	Mass Flow Rate lbs/hr	Pressure Drop Δp psia	h_{avg} Btu/hr ft^2 $^{\circ}F$	$N_{Nu} = \frac{hd}{K}$	$\frac{\Delta p}{(L/D)}$	Condition of Refnt. Entering Evaporator. x_i	Condition of Refnt leaving evaporator x_o
1	65	94.8	1.0	560	278	1.287	0.1	0.63
2	(53.$^{\circ}F$)	67.5	0.62	366	173	0.797	0.13	0.56
3		20.0	0.185	185	92	0.238	0.18	0.52
4		5.16	0.105	59	29.4	0.120	0.3	0.58
1	70 (58)	119	1.26	671	350	1.62	Subcooled $3^{\circ}F$	0.46
2		83.5	0.901	517	270	1.163	0.05	0.48
3		21.5	0.185	108	56.2	0.238	0.12	0.55
1	75	24.6	0.193	124	67	0.248	0.72	0.99
2	(62)	23.75	0.193	116	62.5	0.248	0.76	2°superheat
3		17.3	0.165	100	50.5	0.212	0.8	1.8 superheat
4		16.2	0.158	71	38.4	0.195	0.85	dry and sat
1	77 (64)	18.2	0.187	102.5	89.0	0.241	0.57	0.92
1	80 (66)	38.3	0.56	508	283	0.695	Subcooled $0^{\circ}F$	0.78
2		33.5	0.53	435	242	0.682	Subcooled $5^{\circ}F$	0.59
3		30.2	0.13	217	121	0.62	0.62	Dry and sat.
1	81 (67)	22.2	0.271	217	123	0.348	0.65	0.78

1	2	3	4	5	6	7	8	9	10
7		83	44	0.62	624	265	0.708	0.265	0.98
		(60)	28.2	0.31	208	119	0.392	0.365	0.89
8		85	72.6	1.79	724	419	2.31	5° sub-cooled	0.86
		(70)	37.8	0.552	397	230	0.71	0.1	0.93
			37.4	0.486	371	215	0.625	0.15	0.89
			29.6	0.447	327	189	0.575	0.14	0.73
			18.8	0.303	248	143	0.39	0.23	0.97
			15.4	0.253	207	120	0.325	0.3	0.82
			13.4	0.233	170	98	0.30	0.34	0.78
9		86	54.3	0.363	216	127	.44	0.53	0.9
		(72.5)							
10	1	89	39.5	0.60	445	262	0.772	0.15	0.09
	2	(73°F)	61.5	0.66	359	212	0.85	0.45	0.96
11	1	90	44.7	0.618	360	226	0.795	0.39	0.0
	2	(74)	17.3	0.37	327	195	0.475	Sub-cooled 1° F	dry & cot.
12	1	93	28.2	0.485	299	181	0.625	0.29	0.80
	2	(76)	30.9	0.34	213	129	0.435	0.57	0.93
13	1	95	37.0	0.568	301	185	0.73	0.48	0.96
	2	(77.5)	20.1	0.378	245?	150	0.480	0.23	0.86
	3		16.4	0.32	195	120	0.374	0·32	0·65
	4		13.9	0.265	168	90	0.34	0·4	0·79
	5		9.02	0.218	131	80	0.28	0·4	0·83
	6		6.52	0.114	61.5	38	0.167	0.65	0.85

1	2	3	4	5	6	7	8	9	10
14		97 (79)	62.5	0.862	401	248	1.13	0.59	0.97
15	1	98	60.7	0.990	574	355	1.27	0.44	0.99
	2	(79.5)	14.8	0.21	137	85	0.27	0.68	0.90
16	1	100	9.33	0.233	190	119	0.31	Sub-cooled	0.76
	2	(81)	23.8	0.24	122	76	0.306	5.5° 0.59	0.7
17	1	102 (82)	27.1	0.307	186	118	0.395	0.73	0.99
18	1	103	34.8	0.49	276	174	0.63		
	2	(83)	31.9	0.47	323	204	0.605	0.38	0.99
19	1	105 (84)	58.4	0.761	427	272	0.978	0.45	0.985
20	1	109 (86.5)	32.3	0.272	148	95	0.35	0.85	0.99
21	1	110 (87)	39.5	0.885	486	315	1.1	0.13	0.98
22	1	116 (91)	30.2	0.54	299	195	0.695	0.49	0.93
23	1	120 (93)	66.2	0.883	517	344	1.14	0.47	0.975

TABLE A-2

RESULTS FOR EVAPORATOR TUBE INCLINED AT SMALL ANGLES TO HORIZONTAL EVAPORATOR

PRESSURE - 95 Psia.

Run No	Tube Angle with Horizontal degrees	Mass Flow Rate lbs/hr.	Test Section Heat Input Btu/hr	q/A Btu/hr ft^2	Average Temp Diff. Between Tube Wall & Refnt T_x °F	Condition of Refnt Entering Test Section x_i	Condition of Refnt. Leaving Test Section	Average heat Transfer Coeffi h Btu/hr.ft^2°F
1	2	3	4	5	6	7	S^{E}o	D
1	0	20	542	1182	6.5	0.2	0.07	183
2	0	20	766	1672	7.5	0.15	0.00	223
3	0	20	1080	2355	8.8	0.10	2° superheat	268
4	0	20	1124	2450	9.0	0.09	2° -do	272
5	0	40	542	1182	5.6	0.4	0.64	212
6	0	40	1080	2355	7.2	0.2	0.67	327
7	0	40	1450	3170	8.7	0.15	0.77	363
8	0	40	1930	4220	10.6	0.19	2° superheat	398
9	0	60	542	1182	4.35	0.4	0.57	271
10	0	60	1080	2355	6.35	0.4	0.72	372
11	0	60	1930	4220	9.5	0.32	0.87	445
12	0	60	2935	6400	12.6	0.10	0.93	508
13	0	60	3475	7580	13.8	2°sub-cooled	0.97	548
14	0	80	542	1182	3.7	0.24	0.36	320
15	0	80	1080	2355	5.5	0.20	0.42	428
16	0	80	1930	4220	8.3	0.16	0.56	509

contd---

1	2	3	4	5	6	7	8	9
17	80	80	2935	6400	10.9	0.24	0.85	567
18	0	80	3475	7580	12.1	0.16	0.80	625
19	5	20	542	1182	6.6	0.2	0.67	179
20	5	20	766	1672	7.8	0.15	0.80	217
21	5	20	1080	2355	9.0	0.10	2°sup-orheat	262
22	5	20	1124	2450	9.2	0.08	2°-do-	266
23	5	40	542	1182	5.7	0.4	0.64	207
24	5	40	1080	2355	7.4	0.2	0.67	318
25	5	40	1450	3170	9.0	0.15	0.77	352
26	5	40	1930	4220	10.0	0.19	2° sup-er heat	387
27	5	60	542	1182	4.65	0.4	0.57	200
28	5	60	1080	2355	6.5	0.4	0.72	362
29	5	60	1930	4220	9.7	0.32	0.67	635
30	5	60	2935	6400	13.7	0.18	0.93	493
31	5	60	3475	7580	14.1	2° sub-cooled	0.07	536
32	5	80	542	1182	3.8	0.24	0.36	311
33	5	80	1080	2355	5.7	0.20	0.42	411

Contd.../

1	2	3	4	5	6	7	8	9
34	5	80	1930	4220	8.6	0.16	0.58	490
35	5	80	2935	6400	11.4	0.24	0.85	561
36	5	80	3475	7580	12.2	0.16	0.89	598
37	10	20	542	1182	6.9	0.2	0.07	171
38	10	20	760	1672	8.2	0.15	0.60	204
39	10	20	1080	2355	9.5	0.10	2°sup-orheat	248
40	10	20	1124	2450	9.6	0.08	2°-sb-	250
41	10	40	542	1182	6.0	0.40	0.04	197
42	10	40	1080	2355	7.8	0.20	0.67	302
43	10	40	1450	3170	9.4	0.15	0.77	337
44	10	40	1930	4220	11.8	0.10	2°sup-or heat	358
45	10	60	542	1182	6.8	0.40	0.57	246
46	10	60	1080	2355	8.8	0.40	0.72	346
47	10	60	1930	4220	10.1	0.32	0.87	417
48	10	60	2935	6400	14.4	0.10	0.93	462
49	10	60	3475	7580	14.9	2°sub-cooled	0.97	510
50	10	80	542	1182	6.0	0.24	0.36	295
51	10	80	1080	2355	8.0	0.20	0.42	392
52	10	80	1930	4220	9.1	0.16	0.58	464
53	10	80	2935	6400	12.1	0.24	0.85	530
54	10	80	3475	7580	13.5	0.16	0.89	561

TABLE A-3

DISTRIBUTION OF SURFACE TEMP AND LOCAL HEAT TRANSFER COEFFICIENT ALONG THE LENGTH OF TEST SECTION (HORIZONTAL)

Length of Test Section 3.5 ft. Mean Temp. of Inlet 70°F

Evaporator Pressure = 85 psia

Run No	Mass Flow Rate lbs/hr	q/A Btu/hr ft²°F		Distance from Inlet of Test Section (ft) 0.25 B	0.25 T	0.75 A	1.25 B	1.25 T	1.75 A	1.75 T	2.25 B	2.75 A	2.75 T	3.25 B
1.	73.0	6640	Tube Surface Temp °F	83	80.5	81	81.5	82	82	83	82.5	82	82	81
			Local h Btu/hr.ft²°F	854	812.0	775	741	711	658	658	633	711	711	775
2.	37.0	4050	Tube Surface Temp.	78.5	79.0	79.5	80.5	81.0	81	81.5	81	81	80.5	79.5
			Local h Btu/hr.ft²°F	481	454	420	390	371	371	358	371	371	380	420
3.	22.0	2300	Tube Surface Temp. °F	75.5	76	77	77.5	78	78	78.5	77.5	77	79.0	75.5
			Local h Btu/hr.ft².F	418	322	337	305	300	303	300	306	327	352	418
4.	12.0	1500	Tube Surface Temp °F	75	75.5	75.5	76	76.5	77	77	76.5	75.5	75.0	76
			Local h Btu/hr ft.²F	303	274	274	251	252	216	216	252	274	274	303

TABLE A

DISTRIBUTION OF LOCAL HEAT TRANSFER COEFFICIENTS AND SURFACE TEMPERATURE ALONG THE EVAPORATOR TEST SECTION

EVAPORATOR PRESSURE 75 psia. SAT TEMP. 63 °F

O.N	Mass flow rate lbs/hr.	Q/A Btu/hr ft². F		Distance from Inlet of Evaporator (ft) 0.25 B	0.25 T	0.75 A	1.25 B	1.25 T	1.75 A	2.25 B	2.25 T	2.75 A	3.25 B	3.25 T
1	24.0	600	Tube surface Temp. F	67	68	68.6	68.6	69	69	69.3	69.5	70	70	70.2
			Local h Btu/hr. ft² F.	178	[illegible]	137	127	127	127	127	119	111	111	109
2	23.75	712	Tube surface Temp F	66	67	67.2	67.3	67.7	68.0	68	68.3	68.7	69.6	69.8
			Local h Btu/hr. ft² F.	178	[illegible]	137	134	126	115	110	110	103	95	95
3	17.0	400	Tube Surface Temp. F	65	66.5	66	66	66.5	67	67	67.3	67.3	67.7	67.7
			Local h Btu/hr. ft² F.	161	123	121	121	107	97	97	91	91	86	85
4	13.2	380	Tube surface Temp. F	65	66.5	65.7	65.7	66.2	66.7	67	67.3	67.3	67.5	67.6
			Local h Btu/hr. ft² F.	109	94	80	69	73	70	66	62	62	60	60

TABLE A-5

Distribution of Surface Temp. and Local Heat Transfer Coefficient along the Test Section(Inclined 5° to Horizontal)

q/A = 2355 Btu/hr ft^2, Evaporator Pressure 95 psia, Sat. Temp. 77.5°F

S. No	Mass Flow Rate lb/hr		Distance from Inlet of Test-section (ft)								
			0.75			1.25			1.75		
			A	B	T	A	B	T	A	B	T
1	20	Tube surface Temp °F	83	84	84.5	85	86	86.5	86	86.5	86.5
		Local h Btu/hr.ft^2°F	427	362	336.0	314	277	262.0	324	314.0	205
2	40	Tube surface Temp °F	82	83	84	84.5	86	86.5	86.0	85.0	84.0
		Local h Btu/hr.ft^2 °F	523	427	362	336	277	262	277	314	362
3	60	Tube surface Temp	82	82.5	83	84	84.5	85	85	84	84.5
		Local h Btu/hr.ft^2 °F	523	470	427	362	336	314	314	362	336
4	80	Tube surface Temp	81	81.5	82	83	83.5	84	84	84	83.5
		Local h Btu/hr.ft^2°F	672	588	523	427	392	362	362	362	392

Table A.6

DISTRIBUTION OF SURFACE TEMP AND LOCAL HEAT TRANSFER COEFFICIENT ALONG TEST SECTION (INCLINED AT 10^0 TO HORIZONTAL) MASS FLOW RATE 40 lbs/hr, EVAPORATOR PRESSURE 95 PSIA , SAT TEMP 77.5^0F.

S.No	q/A Btu/hr ft^2		Distance from inlet of test section (ft)								
			0.75	1.25		1.75		2.5	2.75		3.25
			A	B	T	A	B	T	A	B	T
1	1182	Tube surface Temp ^{0}F	80.5	81	81.5	81.5	82	82	82	81.5	82
		Local h Btu/hr.ft^2	394	338	296	296	263	263	263	296	263
2	2355	Tube surface Temp ^{0}F	83	84	84.5	85.5	86	87	86	84	85
		Local h Btu/hr ft^{2}F	428	362	336	296	277	248	277	336	316
3	3170	Tube surface Temp ^{0}F	84.5	85	86	87.5	88.5	88.5	87.5	85.5	86.5
		Local h Btu/hr.ft^2 ^{0}F	453	422	373	317	288	288	317	390	352
4	4220	Tube surface Temp ^{0}F	86.5	87.5	86.5	89	89.5	90	90.5	91	91
		Local h Btu/hr.ft^2 ^{0}F	470	422	384	367	352	338	325	313	313

APPENDIX-B

SAMPLE CALCULATIONS.

Note:- The calculations have been done by using P.H. Chart for Freon$_{-12}$.

Sample Calculation for Horizontal Tube.

Table A.1 Set No.8, Run No.2

Evaporator tube length 3.5 ft, I.D. = 3/8", O.D = $\frac{1}{2}$"

Evaporator pressure = 65 psia.

Saturation temperature= 70°F

Temperature of F_{-12} entering the preheater = 63.5°F

Temperature of F_{-12} leaving the after-heater= 72°F.

Power factor for Test Section = 0.95

Power factor for Preheater = 0.90

Power factor for After-heater = 0.90

Current flowing through test section. = 115 amps.

Voltage drop across test section = 5.06 volts.

∴ Test section Input = 115 x 5.06 x 0.95 x 3.41

= 1072 Btu/hr.

and T.S. Heat Flux, $q/A = \frac{1872 \times 12}{\pi 0.5 \times 3.5} = 4090$ Btu/hr ft^2

Current flowing through Pre-heater = 48 amps.

Voltage drop across the Pre-heater = 2 volts.

∴ Preheater Input = 2 x 48 x 0.9 x 3.412

= 295 Btu/hr.

Current flowing through after-heater = 38 amps.

Voltage drop across after-heater = 1.57 volts.

∴ After heater Input = 1.57 x 38 x 0.9 x 3.412

= 183 Btu/hr.

Total heat supplied = 1872 + 295 + 183

= 2350 Btu/hr.

Enthalpy of refrigerant at 85 psia and 69.5°F = 22.5 Btu/lb.

Enthalpy of refrigerant at 85 psia and 72°F = 84.7 Btu/lb

Assuming no heat losses for the temperature range involved,

$$\text{Mass flow rate} = \frac{2350}{(84.7 - 22.5)} = 37.8 \text{ lbs/hr.}$$

Preheater Input /lb of refrigerant = $\frac{295}{37.8}$

= 7.8 Btus

∴ Enthalpy of refrigerant entering T.S. = 22.5 + 7.8

= 30.3 Btu/lb.

Hence dryness fraction of refrigerant entering T.S. $x_1 = 0.1$

Test section Input/lb of refrigerant = $\frac{1872}{37.8}$

= 49.5 Btu

∴ Enthalpy of refrigerant leaving the T.S. = 30.3 + 49.5

= 79.8 Btu.

Hence dryness fraction of refrigerant leaving T.S., $x_0 = 0.93$

At 70°F Saturation temperature.

Specific heat of liquid B_{12}, C_L = 0.231

Surface tension of liquid[32] R_{12}, σ_L σ = 299,000 lbm/hr^2

Thermal conductivity of liquid[31] R_{12} K_L = 0.054 Btu/hr ft^{0}F

Dynamic viscosity of liquid[31] R_{12} μ_L = 0.0633 lbm/ft.hr

Latent heat of vaporization, h_{fg} = 60.309 Btu/lb.

Average temperature difference between tube surface and liquid refrigerant, T_x = (80.3 - 70)

= 10.3^{0}F

Density of liquid refrigerant, ρ_L = 82.717 lbs/cubic ft.

Density of vapour refrigerant, ρ_V = 2.091 lbs/cubic ft.

Now,

$$\frac{C_L \Delta T_x}{h_{fg}} = \frac{0.231 \times 10.3}{60.309}$$

$$= 0.0395$$

$$\frac{q/A}{h_{fg}} \sqrt{\frac{\sigma}{g(\rho_L - \rho_V)}} = \frac{4090}{3600 \times 0.0633 \times 60.309} \times \sqrt{\frac{299.000}{32.2 (82.72 - 2.09)}}$$

$$= \frac{4090 \times 10.72}{3600 \times 0.0633 \times 60.309}$$

$$= 0.322$$

$$N P_r = \frac{C_L \mu_L}{K_L} = \frac{0.231 \times 0.0633}{0.054} = 2.708$$

$$(NP_r)^{1.7} = (2.708)^{1.7}$$

$$= 5.45$$

$$\frac{C_L \Delta T_x}{h_{fg}} \times \frac{1}{(NP_r)^{1.7}} = \frac{0.395}{5.45}$$

$$= 0.00725$$

Pressure Drop in Evaporator.

Difference between Hg limbs of manometer = 1.12"

∴ Pressure drop, ΔP = (1.12 x .492)

= 0.552 psia

& , $\frac{\Delta P}{(L/D)} = \frac{0.552 \times 0.375 \times 144}{3.5 \times 12}$ psf.

= 0.71 lbs/ft.^{2}

Average heat Transfer Coefficient, have

$$h_{ave} = \frac{q/A}{\Delta T_x} = \frac{4090}{10.3}$$

= 397 Btu /hr ft^2 ^oF

$$N_{Nu} = \frac{h_{ave}\ d}{K_L}$$

$$= \frac{397 \times 0.375}{12 \times 0.054}$$

= 230

Local Heat Transfer Coefficients:

At a distance of 0.75 ft. from entrance,
tube surface temp = 79.5°F

∴ Local ΔT_x = (79.5 - 70) = 9.5° F

$$\text{Local } h = \frac{q/A}{\Delta T_{x \text{ local}}} = \frac{4090}{9.5}$$

= 430 Btu/hr.ft^2

Other coefficients have been calculated in Table A-3 Run No.2.

Calculations for Inclined Tube.

Table A-2, Run No.28

Evaporator pressure = 95 psia. saturation temp.77.5 °F

Tube Angle 5° to horizontal

∴ Mass flow rate = 60 lbs/hr.

Temperature of refrigerant entering preheater = 75°F

Temperature of refrigerant leaving afterheater=78° F

Enthalpy of refrigerant entering preheater = 25 Btu/lb.

Enthalpy of refrigerant leaving afterheater = 85.3 Btu/lb.

∴ Total heat Input = 60 x (85.3 - 25)

= 3618 Btu/hr.

Current flowing through T.S. = 86 amps.

Voltage drop across T.S. = 3.78 volts.

∴ Input = 86 x 3.78 x .95 x 3.412

= 1080 Btu/hr.

or $q/_A$ = $\frac{1080}{.458}$

= 2355 Btu/hr ft^2

Current flowing through preheater = 4.5 amps.

Voltage drop across the preheater = 100 volts.

Preheater Input = 4.5 x 100 x 0.9 x 3.412

= 1500 Btu/hr.

Current flowing through after heater = 3.88 amps.

Voltage drop across the after-heater. = 94 volts.

After heater Input = $\frac{3.88 \times 94 \times 0.9 \times 3.412}{}$

= 1020 Btu/hr.

Assuming no heat losses for the temperature range involved.

Enthalpy of refrigerant entering T.S. = 25 + $(\frac{1500}{60})$

= 50 Btu/lb.

Hence, dryness fraction of refrigerant entering T.S. x1 = 0.4

Similarly enthalpy of refrigerant leaving the T.S.

= 50 + $(\frac{1020}{60})$

= 68 Btu/lb.

Hence, dryness fraction of refrigerant leaving T.S.,x_o=0.72

Average temperature difference between tube surface and refrigerant ΔT_x = (84-77.5) = 6.5°F

$$\therefore h_{ave} = \frac{q/A}{\Delta T_x} = \frac{2355}{6.5}$$

$$= 362 \text{ Btu/hr ft}^2 {}^\circ\text{F}$$

Local heat transfer coefficients.

At a distance of 0.75 from evaporator entrance tube temp = 82°F

$$\therefore \Delta T_x = (82 - 77.5)$$

$$= 4.5^\circ\text{F}$$

$$\therefore h_{Local} = \frac{2355}{4.5}$$

$$= 523 \text{ Btu/hr sq ft}^\circ\text{F}$$

other coefficient have been calculated in table A-5.

REFERENCES

1. FARBER E.A. AND SCORAH R.L. "Heat Transfer of Water boiling under pressure ASME Trans. 70 P.369-84(1948).

2. McADAMS W.H. " Heat Transfer from single horizontal wires to boiling water" Chem.Engg.Prog.44 639-44(1948).

3. NOVAK ZUBER " Nucleate boiling the region of isolated bubbles and similarity with natural convection" Int. J.Heat and Mass Transfer Vol. 6 No.1 p.53-78.

4. K.YAMAGATA AND K. NISHIKAWA " On Correlation of nucleate boiling heat transfer" Int. J.Heat and Mass Transfer 1,219 (1960).

5. DAVIDSON AND AMICK " Formation of gas bubbles at horizontal orifices". Am. Inst.Chem.Engrs. J.2.336(1956).

6. HSU S.T. "Engineering Heat Transfer" D.Van Nostrand Company, Inc. 1963.

7. CRYDER D.S. AND FINALBORGO A.C. " Heat Transfer from metal surfaces to boiling liquids" Trans. Am.Inst. Chem.Engrs. Vol. 33 P. 346 (1937).

8. ROHSENOW W.M. AND CLARK J.A. "A study of Mechanism of boiling heat transfer" ASME Trans. 73: 609-20(1951).

9. ROHSENOW W.M. "A method of Correlating heat transfer data for surface boiling of liquids ASME Trans.Vo.74. 709-75 (1952).

10.GUNTHER F.C. AND KREITH F. "Photographic study of bubble formation in heat transfer to sub-cooled water" P.113. Heat Transfer and Fluid Mechanics Institute, Calif. 1949.

11. Gunther F.C. "Photographic study of surface boiling heat transfer to water with forced convection" Trans.ASME Vol.73, No.2 P.115 Feb. 1951.

12. BRYAN W.L. AND L.G.SIEGAL " Heat Transfer Coefficients in Horizontal tube evaporators" Refrigerating Engg. Vol. 63. May, 1955.

13. MERL BAKER " Heat Transfer rates from heated horizontal tube to Freon$_{-12}$" Refrigerating Engg. Jan . 1956.

14. T.Hara " The mechanism of nucleate boiling Heat Transfer" Int. J. Heat and Mass transfer Vol. 6 No.11(1963).

15. P.Gorse-Schmidt. " Some characteristics of flow patterns and Heat Transfer of Fr$_{-12}$ evaporating in horizontal tubes" Journal of Refrigeration March/April,1960 p.40.

16. R.J.Murray "Local Heat Transfer Coefficient in horizontal tube evaporators" Journal of Refrigeration 1959 p. 118.

17. FRANK O. GASKILL " Evaporator heat transfer analysis Refrigerating Engineering Sept. V. 26 1933 P.126.

18. RATIANI G.V. AND AGALIANI D.V. " Heat Transfer to boiling refrigerants 12 and 22" ASHRAE Journal to Dec. 1963.

19. MARTIN W.H. "Heat Transfer Coefficient in boiling refrigerant" Ref.Engg. Sept. 1938 p.175.

20. McAdams W.H. , W.K.Wood, and W.L. Bryan "Vaporization inside Horizontal Tubes" ASME Trans.Vol.63, p.545 (1941).

21. ASHLEY C.H. "HEAT Transfer of Evaporating Freon$_{-12}$" Ref.Engg.Vol.43 Feb 1942. P.89.

22. WITZIG W.F., G.M. PENNY AND J.A. CYPHERS " Heat Transfer rates to evaporating Freon$_{-12}$ in a horizontal tube evaporator" Ref.Engg. vol.56 August, 1948 P.153.

23. LARSON R.L., G.W. QUAINT AND W.L.BRYAN "Effect of turbulent promotors in Refrigerant Evaporator Coils Refrigerating Engg. Dec. 1949.

24. YODER R.J. AND D.F. DODGE" Heat Transfer Coefficients of Boiling Freon$_{-12}$" Refrigerating Engg. Vol.60 Feb. 1952.

25. BRYAN W.L., G.W.Quaint, "Heat Transfer Coefficient in Horizontal tube evaporator" Refrigerating Engg. Jan, 1951.

26. DANIEL, ..., Y.S. TOULOUKIAN AND G.A.HAWKINS "Heat Transfer film coefficient for refrigerants boiling inside tubes" Refrigerating Engg.Sept. 1953.

27. ALTMAN NORRIS AND STAB " Heat Transfer and Pressure drop of Refrigerants boiling in horizontal evaporator" Journal of Heat Transfer August, 1960.

28. G.POLKE "Evaporation of Refrigerant-12 inside horizontal tubes ASHRAE Journal July, 1963.

29. FRANK KREITH "Principle of Heat Transfer".

30. HARTNETT J.P. "Recent Advances in Heat and Mass Transfer" P. 338 (1961).

31. ASHRAE JOURNAL 1960.

32. HAND BOOK OF CHEMISTRY 10th edition.

33. HANDBOOK Mc ADAMS " HEAT TRANSMISSION" McGraw-Hill Book Company 3rd Edition.

34. JAKOB M. "Heat Transfer" Vol. I Chapter 29, John Wiley and Sons, Inc. Newyork 1949.

35. Bo- PIERRE " The Coefficients of Heat Transfer for Boiling Fr.. in Horizontal Tube " S.F. Review Vol No 2, no 1 1955 P.55-59